university of groningen

University Medical Center Groningen

University of Groningen

Pumping a Ring-Sliding Molecular Motion by a Light-Powered Molecular Motor

Yu, Jing-Jing; Zhao, Li-Yang; Shi, Zhao-Tao; Zhang, Qi; London, Gabor; Liang, Wen-Jing; Gao, Chuan; Li, Ming-Ming; Cao, Xiao-Ming; Tian, He

Published in:
Journal of Organic Chemistry

DOI:
10.1021/acs.joc.9b00783

IMPORTANT NOTE: You are advised to consult the publisher's version (publisher's PDF) if you wish to cite from it. Please check the document version below.

Document Version
Publisher's PDF, also known as Version of record

Publication date:
2019

Link to publication in University of Groningen/UMCG research database

Citation for published version (APA):
Yu, J-J., Zhao, L-Y., Shi, Z-T., Zhang, Q., London, G., Liang, W-J., Gao, C., Li, M-M., Cao, X-M., Tian, H., Feringa, B. L., & Qu, D-H. (2019). Pumping a Ring-Sliding Molecular Motion by a Light-Powered Molecular Motor. *Journal of Organic Chemistry*, *84*(9), 5790-5802. https://doi.org/10.1021/acs.joc.9b00783

Copyright
Other than for strictly personal use, it is not permitted to download or to forward/distribute the text or part of it without the consent of the author(s) and/or copyright holder(s), unless the work is under an open content license (like Creative Commons).

The publication may also be distributed here under the terms of Article 25fa of the Dutch Copyright Act, indicated by the “Taverne” license. More information can be found on the University of Groningen website: https://www.rug.nl/library/open-access/self-archiving-pure/taverne-amendment.

Take-down policy
If you believe that this document breaches copyright please contact us providing details, and we will remove access to the work immediately and investigate your claim.

Downloaded from the University of Groningen/UMCG research database (Pure): http://www.rug.nl/research/portal. For technical reasons the number of authors shown on this cover page is limited to 10 maximum.

Download date: 20-08-2022

JOC The Journal of Organic Chemistry
Cite This: J. Org. Chem. 2019, 84, 5790−5802
Article
pubs.acs.org/joc

Pumping a Ring-Sliding Molecular Motion by a Light-Powered Molecular Motor

Jing-Jing Yu,[†] Li-Yang Zhao,[†] Zhao-Tao Shi,[†] Qi Zhang,[†] Gabor London,[‡,§] Wen-Jing Liang,[†] Chuan Gao,[†] Ming-Ming Li,[†] Xiao-Ming Cao,[†] He Tian,[†] Ben L. Feringa,[†,‡] and Da-Hui Qu*[,†]

[†]Key Laboratory for Advanced Materials and Joint International Research Laboratory of Precision Chemistry and Molecular Engineering, Feringa Nobel Prize Scientist Joint Research Center, School of Chemistry and Molecular Engineering, East China University of Science and Technology, 130 Meilong Road, Shanghai 200237, China

[‡]Centre for Systems Chemistry, Stratingh Institute for Chemistry and Zernike Institute for Advanced Materials, Faculty of Mathematics and Natural Sciences, University of Groningen, Nijenborgh 4, AG Groningen 9747, The Netherlands

[§]Institute of Organic Chemistry, Research Centre for Natural Sciences, Hungarian Academy of Sciences, Magyar, tudósok körútja 2, Budapest 1117, Hungary

Supporting Information

ABSTRACT: Designing artificial molecular machines to execute complex mechanical tasks, like coupling rotation and translation to accomplish transmission of motion, continues to provide important challenges. Herein, we demonstrated a novel molecular machine comprising a second-generation light-driven molecular motor and a bistable [1]rotaxane unit. The molecular motor can rotate successfully even in an interlocked [1]rotaxane system through a photoinduced *cis*-to-*trans* isomerization and a thermal helix inversion, resulting in concomitant transitional motion of the [1]rotaxane. The transmission process was elucidated via ^{1}H NMR, ^{1}H−^{1}H COSY, HMQC, HMBC, and 2D ROESY NMR spectroscopies, UV−visible absorption spectrum, and density functional theory calculations. This is the first demonstration of a molecular motor to rotate against the appreciably noncovalent interactions between dibenzo-**24**-crown-**8** and *N*-methyltriazolium moieties comprising the rotaxane unit, showing operational capabilities of molecular motors to perform more complex tasks.

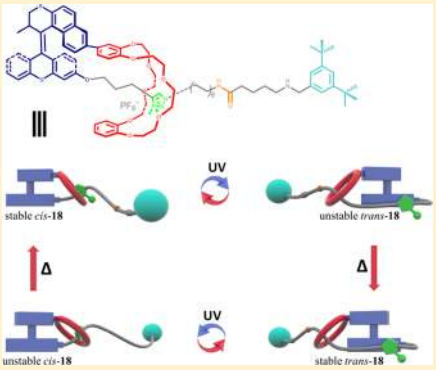

INTRODUCTION

Inspired by biological molecular machines (such as ATPases, kinesin, bacterial flagellar motors, etc.) widely present in nature,[1−3] artificial molecular machines have been successfully constructed by synthetic chemists to mimic the diverse functions of biological systems.[4] Extensive efforts have been focused on the construction, manipulation, and application of artificial molecular machines.[5,6] Diversified molecular machines working at a single-molecule scale or amplifying their motion in a collective manner have been well realized, exhibiting the great significance and possibilities of molecular machines.[7] Biological molecular machines and macroscopic machines have reminded us of the significance to couple two or more machinery operations in a transmission mechanism. Hence, it would be intriguing if such mechanical transmission mechanism could be achieved in the artificial molecular system. Recent efforts have included the successful coupling of the photo-isomerization of azobenzene with mechanical rotation motion,[8] and the coupled intramolecular mechanical transmission from the light-driven unidirectional rotary motion to the synchronous sliding-and-rotation movement of a connected biaryl rotor.[9] These achievements supported strategies and guided inspirations for the design and construction of mechanically coupled artificial molecular machines. However, designing multifunctional mechanical molecular systems remains challenging, especially in addressing the fundamental question of whether we can combine molecular rotary motion with linear sliding motion in a mechanically interlocked system.[10]

Molecular motors are representative classes of molecular machines, which can perform directional rotation under light and heat, have been proven to operate successfully in a variety of environments.[11−14] While rotaxanes are representative classes of mechanically interlocked molecules,[15] in particular, bistable [2]rotaxane based on the noncovalent interactions between the crown ether with ammonium and triazolium stations, have been extensively studied because of their clear shuttling process in response to pH.[16] Herein, our motivation is to integrate these two types of molecular units into a single-molecular system, which would be a great model to explore if molecular motor can operate against the appreciably noncovalent interactions in an interlocked [1]rotaxane, and if the linear motion of the rotaxane can be driven via a transmission

Received: March 25, 2019
Published: April 11, 2019

Downloaded via UNIV GRONINGEN on February 25, 2020 at 15:27:34 (UTC).
See https://pubs.acs.org/sharingguidelines for options on how to legitimately share published articles.

ACS Publications © 2019 American Chemical Society

DOI: 10.1021/acs.joc.9b00783
J. Org. Chem. 2019, 84, 5790−5802

mechanism. Compared to the previously reported [1]rotaxane transmission system,[10] we mainly focus on the operation of molecular motors in interlocking structures, whether the molecular motor can achieve the four-step rotational cycle under the constraint of certain noncovalent interactions, which would provide deeper insight into the operational capabilities of the second-generation molecular motors in more complex mechanical molecular systems. We envision that this research would push the general exploration of multicomponent molecular machines working by coupled motion at the molecular scale, and further give unprecedented insights to the nanoworld.

The envisioned design of a molecular machine with distinct mechanical units allowing transmission of motion, that is, the [1]rotaxane *cis*-**18H**$^+$ molecular motor system, is shown in Figure 1a. A light-driven second-generation molecular motor is

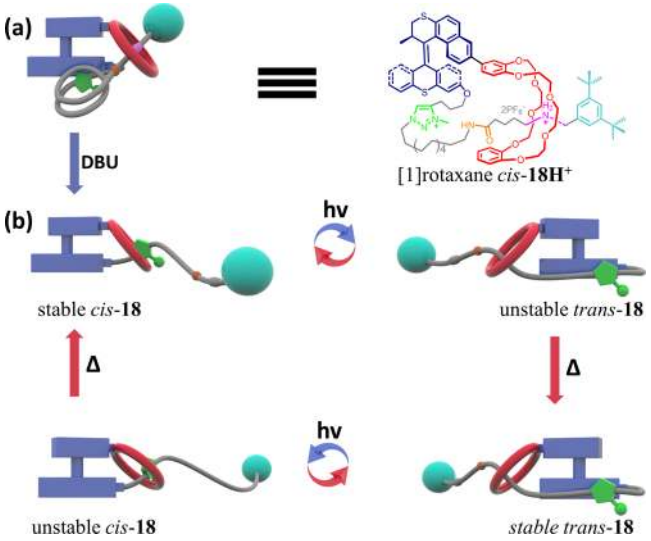

Figure 1. (a) Chemical structures of *cis*-**18H**$^+$ and (b) schematic representation of photo-thermal driven process of [1]rotaxane stable *cis*-**18**. The mechanical transmission cycle is initiated with the deprotonated stable *cis*-**18** by adding base DBU, wherein the **DB24C8** ring locates at the **MTA** sites because of their host−guest combination. UV irradiation drives the first half-cycle rotation of the motor part. This rotation motion further transmits into the **DB24C8** ring, leading to its dissociation with **MTA** sites and subsequent sliding along the long carbon chain, thus yielding unstable *trans*-**18**. Then the THI of the motor unit produces stable *trans*-**18**, and irradiation further drives the second half-cycle rotation, transmitting the sliding motion of the **DB24C8** ring back to the **MTA** site, yielding unstable *cis*-**18**. A second THI from unstable *cis*-**18** to stable *cis*-**18** completes the final step of the one cycle.

covalently immobilized in a [1]rotaxane. The upper rotor part of the motor is modified with a crown ether macrocycle, dibenzo-**24**-crown-**8** (**DB24C8**); and the lower stator part of the motor is connected with a linear thread, which contains two distinguishable recognition sites relative to **DB24C8**, the benzylalkylammonium hexafluorophosphate (**BAA**) station and a *N*-methyltriazolium hexafluorophosphate (**MTA**) station, as well as an auxiliary recognition site, the secondary amide (**SA**) group.[17] The linear component is mechanically threaded into the macrocycle with a bulky 3,5-di-*tert*-butylphenyl group applied as stopper.[18] First, the macrocycle **DB24C8** is stationary at the **BAA** recognition site because of the stronger binding constant[16b,d,e] (Figure 1a). After adding base DBU to the system, the **BAA** station is deprotonated, leading to the movement of the **DB24C8** macrocycle from the **BAA** site to the weaker **MTA** recognition site[16b,d,e] (Figure 1b). Then the stable *cis*-**18** can be transformed into unstable *trans*-**18** via photo-isomerization under UV irradiation (λ = 365 nm). At this moment, the molecular motor would rotate against the host−guest combination of the macrocycle **DB24C8** and guest **MTA**, resulting in the "pulling" process of the **DB24C8** ring away from the **MTA** recognition site. Then the unbound macrocycle is expected to slide along the alkyl chain (**AC**) region near the **SA** group because of the overall molecular configuration (trans motor). After heating (60 °C) the system, unstable *trans*-**18** will undergo a thermal helix inversion (THI) and transform into stable *trans*-**18**, at this stage, the geometry of the entire molecular system basically remains. Continued UV irradiation and heating can trigger the molecular motor to perform a four-step cycle of directional rotation, and the rotor part of the molecular motor would pump the macrocycle slide along the **AC** region to the **MTA** station back and forth, thus realizing a transmission behavior in the bifunctional mechanical system from molecular rotational motion to linear sliding motion. This manner of molecular machinery motion would prove that the molecular motor resists appreciably noncovalent interactions, which has been proven to lock the rotation of a molecular motor in a specific molecular system.[19]

RESULTS AND DISCUSSION

Design. The design of *cis*-**18H**$^+$ is based on the following principles: (i) the S−S molecular motor is selected because of its long half-life at room temperature,[14b,20] which is convenient to track the entire driving process by NMR spectroscopy; (ii) crown ether **DB24C8** is selected because of its flexibility, which might facilitate the mechanical transmission process and the successful full-cycle rotation of the motor unit; (iii) the length of carbon chain between **MTA** station and **BAA** station should be sufficient to provide spatial pathway for the ring-sliding motion, meanwhile enabling the successful THI process to complete the full rotation cycle of the confined molecular motor; (iv) considering that only **MTA** station exists in the system after deprotonation of **BAA** station, in this case, the **DB24C8** ring is hard to leave the current station, it is necessary to introduce another weaker **SA** group to assist the subsequent photothermal-driven process;[17] (v) the **MTA** station is chosen considering the weaker interactions between the **MTA** and **DB24C8** instead of **BAA** station with a high-affinity interaction with the crown ether which would lock the rotation of the molecular motor;[19] (vi) the **BAA** station is still employed to template the rotaxane formation to enable the efficient synthesis of the interlocked structure, and meanwhile the acid/base-responsive capability of **BAA** sites would enable the facile removal of the high-affinity synthesis template by deprotonation.[5h,16d,e]

Synthesis. The synthesis of [1]rotaxane *cis*-**18H**$^+$ is illustrated in Scheme 1. The target *cis*-**18H**$^+$ was divided into three components—molecular motor, **DB24C8** macrocycle, and linear thread. One of the key challenges is to synthesize a bifunctional molecular motor *cis*-**8** with groups at precisely defined positions in stator and rotor to allow rotaxane assembly in such a way the rotary motor function is not compromised. Toward this goal, first a bromine-substituted rotor and a triflate-modified stator were synthesized in multiple steps (detailed are given in Scheme S1). Subsequently, a

DOI: 10.1021/acs.joc.9b00783
J. Org. Chem. 2019, 84, 5790−5802

Scheme 1. Partial Synthesis of [1]Rotaxane *cis*-18H$^+$, NonInterlocked Reference Compound *cis*-21H$^+$ and Corresponding [2]rotaxane 25H$^+$

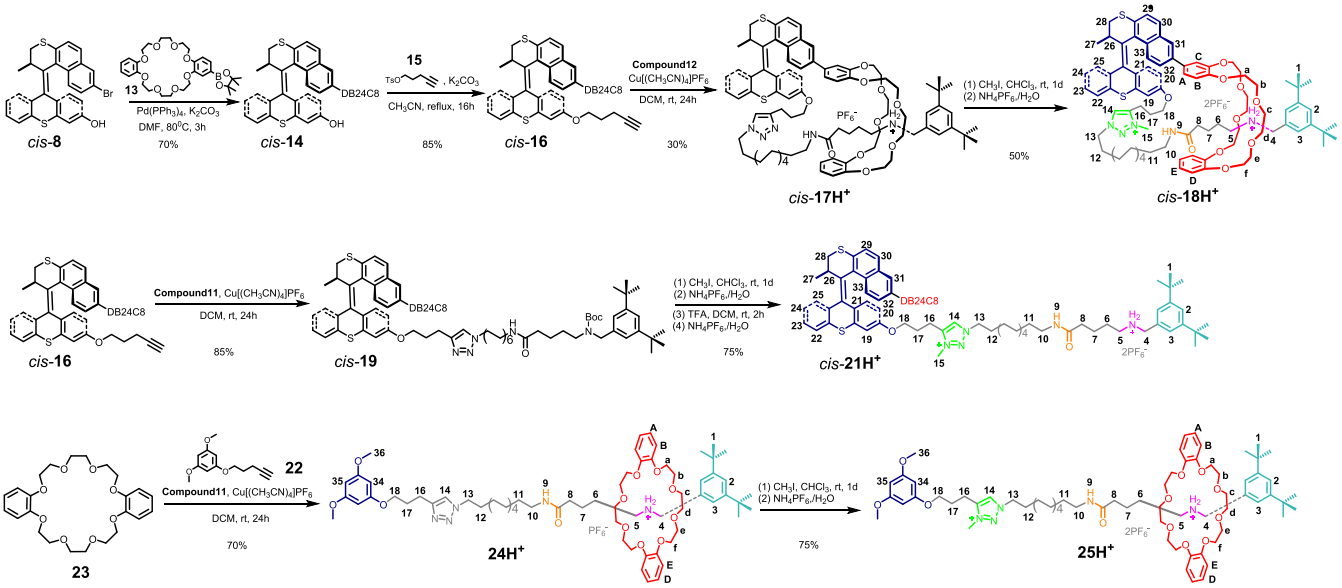

mixture of *cis*-**8** and *trans*-**8** isomers was obtained through Barton−Kellogg diazo-thioketone coupling[21] of thioketone **4** and hydrazone **5** followed by an alkaline hydrolysis reaction. The isomers were separated by flash column chromatography and the structure of *cis*-**8** was confirmed by X-ray single crystal diffraction (Figure S1). Azide-modified linear thread **12** and borate-modified **DB24C8** macrocycle **13** were synthesized by following literature procedures (Schemes S1 and S2). Next, the **DB24C8** macrocycle was mounted to the molecular motor by Suzuki coupling reaction. Alkynyl-substituted *cis*-**16** was obtained by subsequent etherification. Finally, [1]rotaxane *cis*-**17** was obtained through a typical self-threading in apolar solvent, in which a copper(I)-catalyzed Huisgen[5] alkyne−azide 1,3-dipolar cycloaddition was employed to covalently bridge between *cis*-**16** and thread **12**,[22] at this moment, two different configuration isomers of *cis*-**17** generated because the single bond of the naphthalene unit is asymmetrically attached to catechol ring of **DB24C8** (Scheme S2). After a mild methylation reaction by CH_3I, the final [1]rotaxane *cis*-**18H**$^+$ was successfully obtained. Furthermore, the isomer rotaxane *trans*-**18H**$^+$ was synthesized following a similar strategy (Scheme S2). In addition, we also synthesized an non-interlocked reference compound *cis*-**21H**$^+$ and a corresponding [2]rotaxane **25H**$^+$ through a similar synthesis method (Scheme 1). All compounds were fully characterized by ^{1}H NMR, ^{13}C NMR spectroscopy and high-resolution electrospray ionization (HR-ESI).

Structure Verification of [1]Rotaxane *cis*-18H$^+$. To further confirm the structure of [1]rotaxane *cis*-**18H**$^+$, a comparison of the ^{1}H NMR spectra among the interlocked *cis*-**18H**$^+$, noninterlocked *cis*-**21H**$^+$ and the corresponding [2]rotaxane **25H**$^+$ was performed (Figure 2). The characteristic proton signals were assigned by ^{1}H−^{1}H COSY, HMQC, and HMBC (Figures S2−S4, S6, and S12). Compared to the noninterlocked *cis*-**21H**$^+$ (Figure 2a), certain absorptions of *cis*-**18H**$^+$ have split into two groups (Figure 2b), such as proton H_{14} on the **MTA**, aromatic protons H_3, H_{20}, and H_{21}, methyl proton H_{15} and tertiary butyl proton H_1, this is caused by the two different configuration isomers, which are produced during

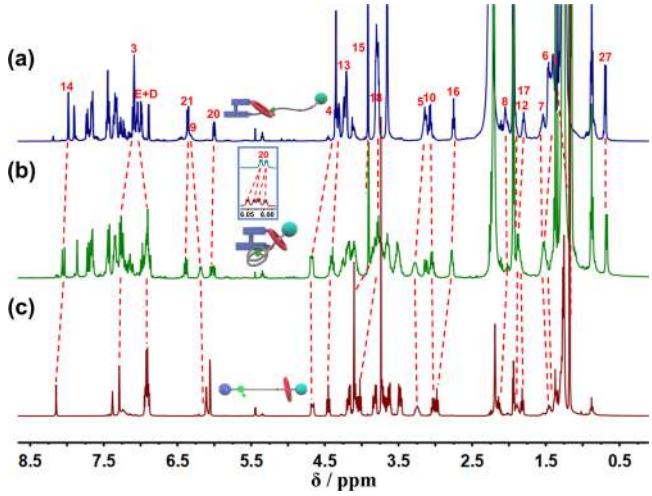

Figure 2. ^{1}H NMR (500 MHz, 298 K, CD_3CN) spectra of (a) noninterlocked reference compound *cis*-**21H**$^+$, (b) [1]rotaxane *cis*-**18H**$^+$ (inset: magnification of proton H_{20}), (c) corresponding [2]rotaxane **25H**$^+$.

the self-threading and "Click Chemistry" reaction (Scheme S2). Distinctive changes of other ^{1}H NMR signals were observed as well, for instance the methylene protons H_4 and H_5 near the **BAA** station shifted downfield ($\Delta\delta$ = 0.33 ppm, $\Delta\delta$ = 0.13 ppm, respectively), which is attributed to the hydrogen-bonding interactions with the oxygen atoms of the crown ether moiety. The amide proton H_9 and the *tert*-butyl protons H_1 shifted upfield ($\Delta\delta$ = −0.17 ppm, $\Delta\delta$ = −0.14 ppm, respectively) because of the shielding effect of the crown ether ring. In addition, a comparison with the corresponding [2]rotaxane **25H**$^+$, which is also an interlocked structure, shows that the ^{1}H NMR signals of protons near the **BAA** station are highly consistent (Figure 2c). The structure of *cis*-**18H**$^+$ was further confirmed by 2D ROESY spectroscopy (Figure S5, S7, and S13) and both *cis*-**18H**$^+$ and [2]rotaxane **25H**$^+$ showed a strong ROEs effect between **DB24C8** and the **BAA** station, while *cis*-**21H**$^+$ did not show any obvious ROEs

DOI: 10.1021/acs.joc.9b00783
J. Org. Chem. 2019, 84, 5790−5802

effect. The combined data clearly indicate that *cis*-**18H**$^+$ features an interlocked [1]rotaxane structure.

Operation of Reference [2]Rotaxane. In order to fully understand the movement of the macrocycle after deprotonation of the **BAA** recognition site. Two distinct reference [2]rotaxane **24H**$^+$ and **25H**$^+$ were synthesized (Schemes 1c and S3). The localization of the **DB24C8** was investigated via ^{1}H NMR spectroscopy (Figure 3b–e). In the initial state, the

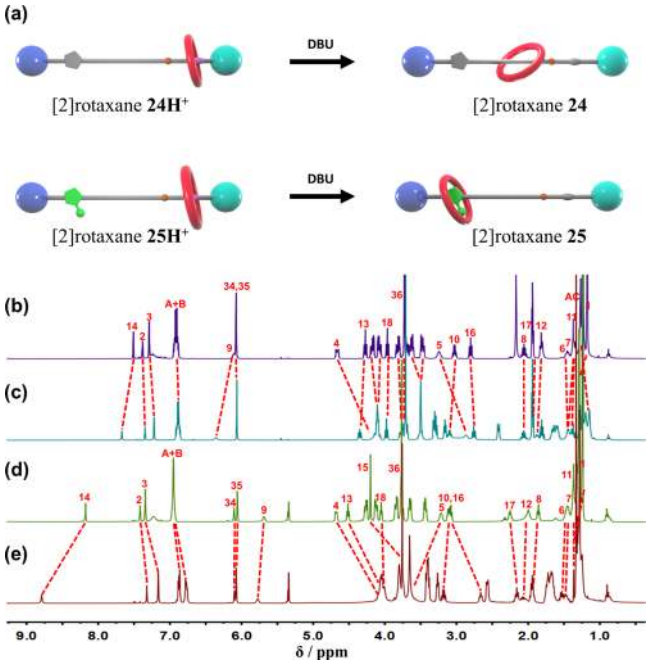

Figure 3. (a) Scheme representation of the DBU-triggered motion of the [2]rotaxane **24H**$^+$ and rotaxane **25H**$^+$; ^{1}H NMR (400 MHz, 298 K, CD_3CN) spectra of (b) [2]rotaxane **24H**$^+$; (c) [2]rotaxane **24** obtained after adding 1.50 equiv of DBU to [2]rotaxane **24H**$^+$; ^{1}H NMR (400 MHz, 298 K, CD_2Cl_2) spectra of (d) [2]rotaxane **25H**$^+$; (e) [2]rotaxane **25** obtained after adding 1.50 equiv of DBU to rotaxane **25H**$^+$.

DB24C8 was located on the **BAA** station (Figures S8, S9, S12, and S13), after addition of DBU to the **24H**$^+$ and **25H**$^+$, respectively, the deprotonated **24** and **25** can be obtained. The obvious changes of ^{1}H NMR spectra between protonated rotaxane **24H**$^+$ and deprotonated rotaxane **24** showed that the **DB24C8** would move off the **BAA** station and was confined in the **AC** region after addition of DBU (Figure 3b,c). Furthermore, the protons H_4 and H_5 near the **BAA** station shifted upfield ($\Delta\delta$ = −0.51 ppm, $\Delta\delta$ = −0.37 ppm, respectively) because they lost their hydrogen bonding interactions with the oxygen atoms of **DB24C8**, while the protons H_1 shifted downfield ($\Delta\delta$ = 0.06 ppm) because of the disappearance of the **DB24C8** shielding effect. Meanwhile, the protons on the **AC** region shifted upfield ($\Delta\delta$ = −0.08 ppm) because of the shielding effect of the **DB24C8**. The protons H_9, H_{10}, H_{11}, H_{12}, H_{13}, and H_{14} expectedly shifted downfield slightly ($\Delta\delta$ = 0.25 ppm, $\Delta\delta$ = 0.07 ppm, $\Delta\delta$ = 0.05 ppm, $\Delta\delta$ = 0.06 ppm, $\Delta\delta$ = 0.08 ppm, $\Delta\delta$ = 0.09 ppm, respectively) ascribed to the deshielding effect of **DB24C8**. In this state, the **DB24C8** ring kept a procumbent configuration, in which the benzene groups of **DB24C8** would be closed to the triazole and the **SA** group. In addition, the protons on the **AC** region showed a strong correlation with the protons on the **DB24C8** ring according to the 2D ROESY spectrum (Figure S11). All the above results confirmed that the **DB24C8** ring moved from the **BAA** station to the **AC** region after adding DBU to the rotaxane **24H**$^+$. Interestingly, this result seems inconsistent with previous work, which indicated that the amide moieties could serve as molecular stations for **DB24C8**[17] The key factor is the weaker binding force between the **SA** group and **DB24C8**, leading to the **DB24C8** ring staying in the **AC** region under thermodynamic control. Similarly, the comparison between the ^{1}H NMR spectra of protonated rotaxane **25H**$^+$ and deprotonated rotaxane **25** shows that the **DB24C8** would move away from **BAA** and combine with **MTA** station after addition of DBU (Figure 3d,e), which is consistent with a typical bistable [2]rotaxane.[16b,d,e] Remarkably, the proton H_{14} on the **MTA** station dramatically shifted downfield ($\Delta\delta$ = 0.61 ppm) because of the deshielding effect from the aromatic rings of the **DB24C8**. Meanwhile, the protons H_{13}, H_{15}, and H_{16} obviously shifted upfield ($\Delta\delta$ = −0.51 ppm, $\Delta\delta$ = −0.45 ppm, $\Delta\delta$ = −0.43 ppm, respectively) because of the shielding effect of the **DB24C8**. The localization of the **DB24C8** was confirmed though 2D ROESY spectroscopy (Figure S15).

The abovementioned results illustrate the movement of the macrocycle in the presence and absence of the **MTA** station. In the presence of a stronger secondary **MTA** recognition site, **DB24C8** would stay at the **MTA** station, whereas in the presence of only a weak **SA** group, the **DB24C8** ring prefers to move to a thermodynamically stable **AC** region. The detailed understanding of the states of rotaxanes, which potentially exist in *cis*-**18H**$^+$, will provide a good experimental basis for the subsequent characterization and analysis of [1]rotaxane *cis*-**18H**$^+$.

Operation of [1]Rotaxane *cis*-18H$^+$. Because the **DB24C8** ring of [1]rotaxane *cis*-**18H**$^+$ is located at the **BAA** station in the initial state, the base DBU needs to be added to the system triggering it to enter stable *cis*-**18**. It should be noted that the ^{1}H NMR spectra of current *cis*-**18H**$^+$ in Figure 4a and the same *cis*-**18H**$^+$ in Figure 2b are not exactly consistent, especially the ratio of doublet H_{14} because they were prepared in different batches, considering that the

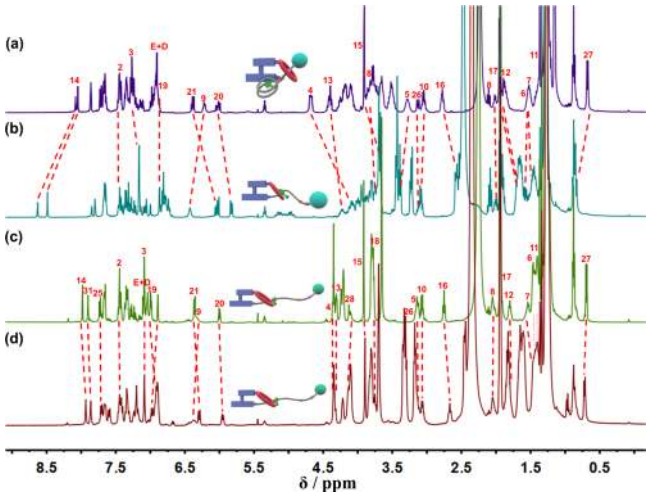

Figure 4. ^{1}H NMR (500 MHz, 298 K, CD_3CN) spectra of (a) [1]rotaxane *cis*-**18H**$^+$; (b) [1]rotaxane stable *cis*-**18** obtained after adding 1.5 equiv of DBU to *cis*-**18H**$^+$; (c) noninterlocked reference compound *cis*-**21H**$^+$; (d) reference compound *cis*-**21** obtained after adding 1.50 equiv of DBU to *cis*-**21H**$^+$.

DOI: 10.1021/acs.joc.9b00783
J. Org. Chem. 2019, 84, 5790–5802

synthesis conditions are difficult to achieve completely consistent, resulting in small differences in the ratio of the two configuration isomers. The comparison of the ^{1}H NMR spectra between protonated *cis*-**18H**$^+$ and deprotonated stable *cis*-**18** confirmed that **DB24C8** could move from the **BAA** recognition site to the **MTA** recognition site after addition of DBU (Figure 4a,b). A large number of protons underwent significant chemical shift changes, which is consistent with the presence of [2]rotaxane **25H**$^+$ (Figure 3d,e). The proton H_{14} shifted downfield ($\Delta\delta$ = 0.11 ppm) because of the hydrogen bonding interaction with the oxygen atoms of the **DB24C8** ring. On the other hand, the protons H_{12}, H_{13}, H_{15}, H_{16}, and H_{17} shifted upfield ($\Delta\delta$ = −0.17 ppm, $\Delta\delta$ = −0.20 ppm, $\Delta\delta$ = −0.24 ppm, $\Delta\delta$ = −0.21 ppm, $\Delta\delta$ = −0.22 ppm, respectively), as a result of the shielding effect of the **DB24C8** ring. The protons H_4 and H_5 near the **BAA** station shifted upfield and downfield ($\Delta\delta$ = −0.59 ppm, $\Delta\delta$ = 0.11 ppm, respectively) because of the departure of the **DB24C8** ring. In particular, the methyl proton H_{27} on the rotor moiety dramatically shifted downfield ($\Delta\delta$ = 0.19 ppm) because the **DB24C8** macrocycle recognized with the **MTA** site, affecting the spatial configuration of the molecular motor (Figure 8). Compared with noninterlocked reference compound *cis*-**21H**$^+$, the ^{1}H NMR signals did not change significantly after addition of DBU (Figure 4c,d). In addition, the **MTA** proton H_{14} of stable *cis*-**18** exhibited a strong ROE effect with **DB24C8** protons (a−f) (Figures S19 and S20). These results unequivocally confirmed that the **DB24C8** ring could move from the **BAA** recognition site to the **MTA** recognition site after addition of DBU.

We hypothesized that the rotational motion of the molecular motor would drive the dissociation of the noncovalent host−guest combination between the **DB24C8** ring and **MTA** recognition site. This process was investigated via ^{1}H NMR spectroscopy (Figure 5) (see partial enlargement in Figures S21−S24). Upon irradiation of UV light at 365 nm for 2 h, stable *cis*-**18** converts into unstable *trans*-**18** because of the photoisomerization (Figure 6a,b) with concomitant change in

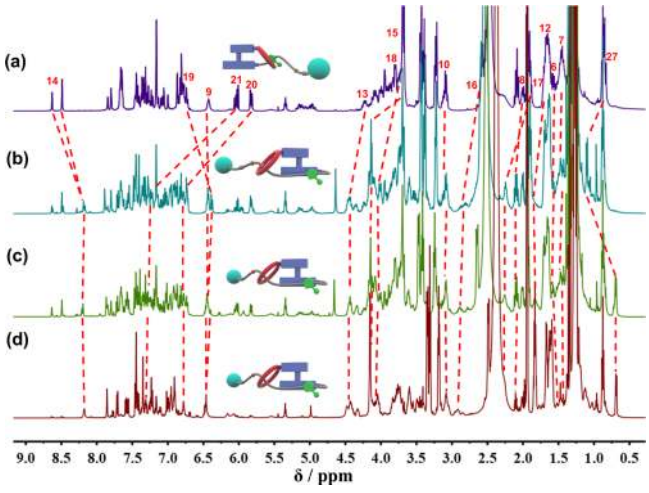

Figure 5. ^{1}H NMR (500 MHz, 298 K, CD_3CN) spectra of (a) [1]rotaxane stable *cis*-**18**; (b) [1]rotaxane unstable *trans*-**18** obtained after stable *cis*-**18** was irradiated with UV (365 nm) for 2 h; (c) [1]rotaxane stable *trans*-**18** obtained after unstable *trans*-**18** was heated at 60 °C for 24 h in the dark; (d) [1]rotaxane stable *trans*-**18** obtained after adding 1.50 equiv of DBU to *trans*-**18H**$^+$.

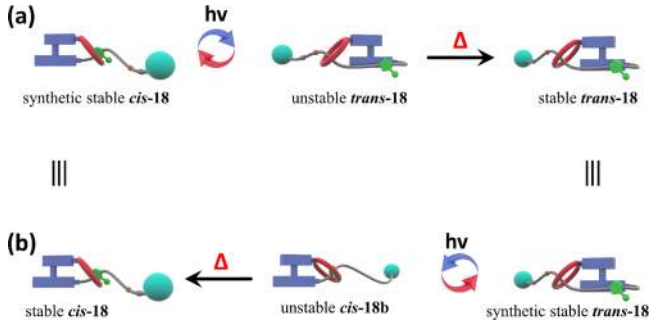

Figure 6. Schematic representation of the photo-thermal driven process of (a) [1]rotaxane stable *cis*-**18** and (b) [1]rotaxane stable *trans*-**18**.

the ^{1}H NMR signals of the protons on the molecular motor. The protons H_{20} and H_{21} obviously shifted downfield (δ = 0.94 ppm, $\Delta\delta$ = 1.28 ppm, respectively), and the proton H_{19} shifted upfield (δ = −0.36 ppm) (Figure S21), which indicated that the shielding effect and the deshielding effect of the naphthalene have been eliminated in the trans isomer. Proton H_{27} shifted downfield (δ = 0.25 ppm) (Figure S24); this chemical shift can be attributed to the increased deshielding effect of the pseudo-equatorial methyl group. Furthermore, the aliphatic protons H_{28} and $H_{28'}$ in the upper-half of the motor shifted upfield (δ = −0.12 ppm, δ = −0.16 ppm, respectively) (Figure S22) because of the difference in the conformational structure of the six-membered ring in stable *cis*-**18** and unstable *trans*-**18**. These results suggest that the [1]rotaxane stable *cis*-**18** has transformed from the stable *cis* state to unstable trans state, was consistent with previous reports.[12b,14b] It is important to note that extended irradiation for 2 h resulted in a photostationary state (PSS) with a ratio of 58:42 (unstable *trans*-**18**/stable *cis*-**18**), calculated by the relative integration of the signals for the methyl group of each isomers. Unsurprisingly, the ratio of two isomers was lower than that in previous reports[12b,14b] because the interlocked [1]rotaxane limited the movement of the molecular motor to some extent. It should be emphasized that the chemical shifts of protons on the thread part also changed significantly. The protons H_{12}, H_{13}, H_{15}, H_{16}, H_{17}, and H_{18} near the **MTA** station were all shifted downfield ($\Delta\delta$ = 0.13 ppm, $\Delta\delta$ = 0.21 ppm, $\Delta\delta$ = 0.46 ppm, $\Delta\delta$ = 0.26 ppm, $\Delta\delta$ = 0.35 ppm, $\Delta\delta$ = 0.34 ppm, respectively) because of the disappearance of the shielding effect from the **DB24C8** ring (Figure S22). Proton H_{14} on the **MTA** station shifted upfield ($\Delta\delta$ = 0.30 ppm) because of the absence of hydrogen bonding interactions with the oxygen atoms of **DB24C8**. These results indicated that **DB24C8** of stable *cis*-**18** is located away from the **MTA** recognition site after illumination. Though the ^{1}H NMR signals of protons H_9 on the **SA** group and H_6, H_7, H_8, and H_{10} near the **SA** group did not change significantly, it is worth noting that the protons on the **AC** region obviously shifted upfield ($\Delta\delta$ = −0.04 ppm) (Figure S23), which could be attributed to the shielding effect of **DB24C8**. Meanwhile, the strong ROE effects between the crown ether hydrogen (a−f) and **AC** region were observed by the 2D ROESY spectrum (Figure S33). The results confirmed that **DB24C8** of stable *cis*-**18** moved from the **MTA** station to **AC** region after UV irradiation, which was consistent with the abovementioned reference [2]rotaxane **24** formed by addition DBU to [2]rotaxane **24H**$^+$ (Figure 3b,c). After heating the unstable *trans*-**18** at 60 °C overnight in the dark, the molecular

DOI: 10.1021/acs.joc.9b00783
J. Org. Chem. 2019, 84, 5790−5802

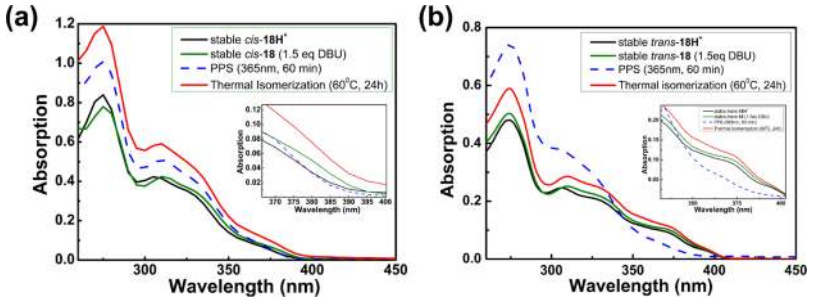

Figure 7. (a) UV−vis absorption spectra (CH_2Cl_2, 283 K) of [1]rotaxane stable *cis*-**18H**$^+$ before and after adding the DBU, UV irradiation for 60 min, heating for 24 h; (b) [1]rotaxane stable *trans*-**18H**$^+$ before and after adding the DBU, UV irradiation for 60 min, heating for 24 h.

motor underwent a THI process from an unstable trans state to a stable trans state. Considering no major structural change between these two states, most signals showed no obvious shift (Figure 5c). However, the H_{28} and $H_{28'}$ on the upper-half of molecular motor-shifted downfield (Figure S22), and the protons H_{27} on the methyl significantly shifted upfield ($\Delta\delta$ = −0.42 ppm) (Figure S24), both of which indicated that the unstable *trans*-**18** had transformed into stable *trans*-**18**. Therefore, the motor of stable *cis*-**18** had been operated successfully for half cycle.

Operation of [1]Rotaxane *trans*-18H$^+$. To further verify the authenticity of the abovementioned half cycle, we synthesized a reference compound *trans*-**18H**$^+$ through a comparable strategy used for *cis*-**18H**$^+$ (Scheme S2). Similarly, the **DB24C8** ring of [1]rotaxane *trans*-**18H**$^+$ located at the **BAA** station in the initial state, after adding the DBU to the system, **BAA** station was deprotonated. As expected, only the methylene protons H_4 near the **BAA** station shifted upfield because of deprotonation ($\Delta\delta$ = 0.24 ppm), the ^{1}H NMR signals of protons in other regions did not change obviously (Figure S34) because the **DB24C8** ring cannot move to the **MTA** recognition site after deprotonation because of the limitation of the spatial structure of stable *trans*-**18**. By comparing the ^{1}H NMR spectra of stable *trans*-**18** obtained from deprotonation of *trans*-**18H**$^+$ and the same stable *trans*-**18** obtained from stable *cis*-**18** after UV irradiation and heating, though some unexpected byproduct accumulated because of sequential isomeric reactions without purification, partial characteristic signal peaks were highly consistent (Figure 5c,d). The results further confirmed that stable *cis*-**18** can be operated according to the set program after illumination and heating. Based on the cumulated data, it can be concluded that the second-generation light-driven molecular motor can resist the considerable noncovalent interactions to allow directional rotation and accomplish a shuttling movement of the rotaxane via a transmission mechanism.

To further prove the complete four-step cycle of stable *cis*-**18**, the solution of stable *trans*-**18** was irradiated under UV (365 nm) for 2 h and subsequently heated at 60 °C for 24 h in the dark. However, the signals of ^{1}H NMR spectra were too complicated to unequivocally assign because of the incomplete photoisomerization and THI processes (Figures S25 and S26). To further explore these two processes, the latter half cycle was accomplished by driving stable *trans*-**18** directly, which was obtained from synthetic *trans*-**18H**$^+$ after adding DBU (Figures 6b and S34). Upon the UV irradiation, the molecular motor stable *trans*-**18** would transform into an unstable *cis* state from a stable trans state. At the meantime, the **DB24C8** ring would move to the **MTA** recognition site because of the decrease of tension in the molecule. Notably, the long and flexible thread component enabled this movement. In this process, the corresponding ^{1}H NMR signals changed significantly (Figure S41a,b), notably, the protons H_{20} and H_{21} dramatically shifted upfield (δ = −0.91 ppm, $\Delta\delta$ = −1.10 ppm, respectively), and the proton H_{19} shifted downfield (δ = 0.35 ppm), and the proton H_{27} obviously shifted downfield (δ = 0.25 ppm), which indicated that the stable *trans*-**18** transformed into unstable *cis*-**18**. Importantly, the proton H_{14} on the **MTA** station dramatically shifted downfield ($\Delta\delta$ = 0.40 ppm) because of the hydrogen bonding interactions with the oxygen atoms of **DB24C8**. Meanwhile the methyl proton H_{15} on the **MTA** station shifted upfield significantly ($\Delta\delta$ = −0.46 ppm), attributed to the shielding effect from the **DB24C8** ring. The protons H_{12}, H_{13}, H_{16}, H_{17}, and H_{18} near the **MTA** station all shifted upfield ($\Delta\delta$ = −0.07 ppm, $\Delta\delta$ = −0.13 ppm, $\Delta\delta$ = −0.23 ppm, $\Delta\delta$ = −0.34 ppm, $\Delta\delta$ = −0.37 ppm, respectively). A clear ROE effect was observed between the protons H_a−H_f of **DB24C8** and H_{14} at the **MTA** station (Figure S43). These results confirm that the **DB24C8** unit of unstable *cis*-**18** have moved from the **AC** region to the **MTA** station after illumination. After heating the solution of unstable *cis*-**18** at 60 °C 24 h in the dark, the molecular motor underwent a THI process from an unstable cis state to a stable cis state. The observed ^{1}H NMR signals were consistent with that of an independent sample of stable *cis*-**18** (Figure S41c,d). The above results proved that in principle, the entire four-step cycle of [1]rotaxane stable *cis*-**18** can be successfully executed.

UV−Vis Absorption Spectroscopy. The photochemical and thermal isomerization processes of the [1]rotaxane *cis*-**18H**$^+$ were furthermore studied by UV−vis absorption spectroscopy in CH_2Cl_2. After adding DBU to the system, a slight red shift in the maximum absorption was observed (Figure 7a), indicating a geometrical change of the molecular motor because of the movement of rotaxane from **BAA** station to **MTA** station. This result provides an explanation for the chemical shift of proton H_{27} after the deprotonation of *cis*-**18H**$^+$ (Figure 4a,b). Upon UV irradiation at 10 °C, the maximum absorption gradually shifted from 382 to 365 nm, which was consistent with increased strain at the central double bond, and hence the generation of a higher-energy unstable isomer. Allowing the solutions to heat to 60 °C for 24 h resulted in a red-shift, which was consistent with thermal isomerization to the corresponding stable isomers. Similar photochemical and thermal isomerization behavior of stable *trans*-**18** was detected using UV−vis analysis (Figure 7b). The dynamic process was consistent with that observed for stable *cis*-**18** (vide supra), and in agreement with the photochemical properties of related molecular motors reported earlier by our

DOI: 10.1021/acs.joc.9b00783
J. Org. Chem. 2019, 84, 5790−5802

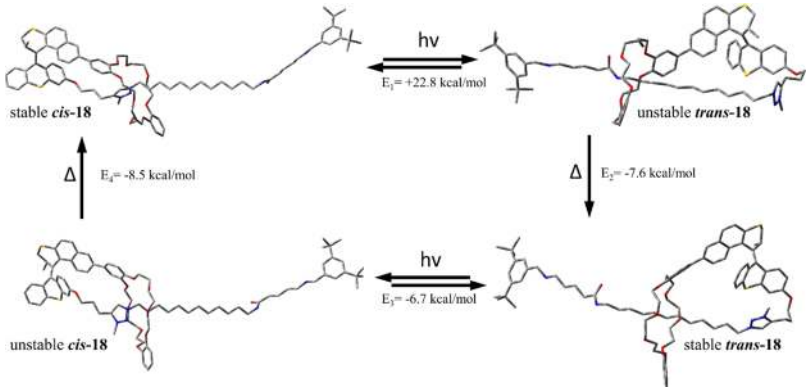

Figure 8. Energy-minimized structures of [1]rotaxane stable *cis*-**18** at four-step cycle optimized using DFT at the RB3LYP/6-311+G (d) level.

group.[11a,12b,14b] The results showed that the rotational motion of the molecular motor unit was not restrained in the mechanically interlocked [1]rotaxane, even in the presence of the rotaxane host−guest interaction.

DFT Calculations. To get a more detailed insight into the entire transmission mechanism of [1]rotaxane stable *cis*-**18** and support the proposed structural changes, the energy optimization states of stable *cis*-**18** in the four-step cycle were calculated by density functional theory (DFT), and all optimizations were performed on the RB3LYP/6-311+G (d) level of theory. The optimized geometries are shown in the Figure 8. The results indicate that the **DB24C8** ring of stable *cis*-**18** is located on the near **MTA** station instead of just above it, which confirm the peculiar changes of proton H_{27} after the protonation of *cis*-**18H**$^+$ (Figure 5b) because movement of the **DB24C8** ring to the **MTA** site would distort the motor molecules. Upon UV irradiation, the stable *cis*-**18** transformed into unstable *trans*-**18**, the optimized geometry showed that the **DB24C8** ring is located on the **AC** region, which is consistent with the aforementioned ^{1}H NMR analysis (Figure 5). Meanwhile the **DB24C8** ring has moved about 14.4 Å compared with the initial position. In this photoisomerization process, the electronic energies increase dramatically (the relative energy ΔE_1 = +22.8 kcal/mol) because of the crowded equatorial orientation of the methyl group in a *trans* configuration. After heating, the unstable *trans*-**18** transforms into stable *trans*-**18**, the molecular motor undergoes a THI, leading to a slightly changed position of the **DB24C8** ring. Simultaneously, the electronic energies decreased because of the recovery of the axial orientation (the relative energy ΔE_2 = −7.6 kcal/mol). In the next stage of the process, stable *trans*-**18** isomerizes into unstable *cis*-**18** upon the UV irradiation, and the **DB24C8** ring returns back to the **MTA** site. Meanwhile, the axial orientation of methyl group transforms into an equatorial orientation, which should be accompanied by an increase in energy, but the energy dramatically decreased (ΔE_3 = −6.7 kcal/mol). This is a reasonable result in view of the formation of the *cis* isomer with more relaxed molecular geometry. After the final THI process, unstable *cis*-**18** converted into stable *cis*-**18**, and the energy further decreased (ΔE_4 = −8.5 kcal/mol) because of the more stable axial orientation of the methyl group. The detailed data of the four-step state were also summarized in Tables S1−S8 and Figures S44−S47. It can be concluded that the variation in energy and stability of the isomers in the light-driven process of stable *cis*-**18** was not only dependent on the change in orientation of methyl,[20a] but is also governed by the entire molecular geometry. Compared to the cis isomers, trans isomers are more distorted resulting in higher energy, which may be another reason for the decrease in ratio of unstable trans isomers and stable cis isomers in the PSS state during the photoisomerization.

CONCLUSIONS

In summary, we have demonstrated the design, characterization and operation of a composite motor-[1]rotaxane contained a light-driven molecular motor and a bistable rotaxane. Detailed NMR experiments and molecular dynamics simulation confirmed that the molecular motor can perform directional rotation, even being integrated with an interlocked [1]rotaxane with considerable noncovalent interactions between macrocycle **DB24C8** and **MTA** recognition sites being present. Demonstrating the complete four-step cycle using interrupted light and heat stimuli, it is evident that unidirectional rotary motion can be transmitted successfully into translational motion. These studies provide deeper insight into the operational capabilities of the second-generation molecular motors in more complex mechanical molecular systems and an important step on our route to explore molecular machines that can perform more complex mechanical tasks.

EXPERIMENTAL SECTION

General Methods and Details. Chemicals were purchased from Acros, Aldrich, TCI, Adamas, or Merck and used as received unless otherwise stated. Solvents were reagent grade, which were dried and distilled prior to use according to standard procedures. All reactions were carried out under an atmosphere of dry argon unless otherwise stated. NMR experiments (^{1}H NMR, ^{13}C NMR, ^{1}H−^{1}H COSY, HMQC, HMBC, and 2D Roesy) were measured on a Brüker AVANCE III 400, AVANCE III 500 or Ascend 600 spectrometer. High-resolution mass spectra (HR-MS) were tested on a LCT Premier XE mass spectrometer by using ESI analyzed by time-of-flight (TOF). The UV−vis absorption spectra and fluorescence spectra were also recorded on a Varian Cary 100 spectrometer and a Varian Cary Eclipse (1 cm quartz cell used), respectively. Photo-driven experiments were carried out by a PerfectLight PL-LED 100 with a constant wavelength of 365 nm. The X-ray diffraction intensity data were collected at 273 or 200 K on a Rigaku RAXIS RAPID IP imaging plate system with Mo Kα radiation (λ = 0.71073 Å). The CIF files for the crystallographic data have been deposited in the Cambridge Crystallographic Data Centre, and the CCDC number is 1882649.

Syntheses of Molecular Motor 8 and Compound 12. *3-Hydroxy-9H-thioxanthen-9-one (2).* To a solution of compound **1**[23] (20 g, 82.6 mmol) in toluene was added anhydrous aluminum trichloride (22 g, 165.2 mmol) slowly. Then the mixture was stirred

DOI: 10.1021/acs.joc.9b00783
J. Org. Chem. 2019, 84, 5790−5802

under reflux with argon atmosphere for 8 h. After the reaction was over, concentrated hydrochloric acid (40 mL) and ice water (60 mL) was added carefully and slowly to quench the reaction. The more ice water (250 mL) was added to the reaction solution, the more mass of white solid was precipitated. The precipitate was filtered under reduced pressure, washing the filter cake with toluene and water, then the white solid was dried under vacuum for 16 h to afford compound **2** (18.8 g, 90%) as a white powder. ^{1}H NMR (400 MHz, DMSO, 298 K): δ (ppm) 10.93 (s, 1H), 8.42 (d, J = 8 Hz, 1H), 8.34 (d, J = 8.8 Hz, 1H), 7.72 (m, 2H), 7.54 (t, J = 6.4 Hz, 1H), 7.06 (d, J = 2 Hz, 1H), 7.01 (dd, J = 8.8, 2 Hz, 1H). ^{13}C{^{1}H} NMR (100 MHz, DMSO, 298 K): δ (ppm) 178.1, 162.0, 139.2, 136.6, 132.9, 132.2, 129.3, 129.0, 127.01, 126.7, 121.4, 116.8, 110.8. HR-MS (ESI-TOF) (m/z): $[M - H]^-$ calcd for $C_{13}H_7O_2S$, 227.0172; found, 227.0177.

*9-Oxo-9H-thioxanthen-3-yl Trifluoromethanesulfonate (**3**).* To a solution of compound **2** (3 g, 13.1 mmol) in anhydrous dichloromethane was added anhydrous pyridine (10.5 mL, 131.0 mmol), then trifluoromethanesulfonic anhydride (5.6 g, 19.8 mmol) was added dropwise under ice bath. After addition, the mixture was stirred at room temperature with argon atmosphere for 16 h. Then the solvent was removed, and the residue was dissolved in dichloromethane (150 mL). The solution was washed with 1 N HCl aqueous solution (100 mL) and brine (100 mL), and then the organic layer was dried over Na_2SO_4 and concentrated in vacuo. The crude product was purified by column chromatography (SiO_2, PE/EA = 100:1) to afford compound **2** (4.7 g, 95%) as a white solid. ^{1}H NMR (400 MHz, $CDCl_3$, 298 K): δ (ppm) 8.71 (d, J = 9.2 Hz, 1H), 8.61 (dd, J = 8.0 Hz, 1.2, 1H), 7.68 (m, 1H), 7.60 (dd, J = 8.0, 0.8 Hz, 1H), 7.54 (m, 1H), 7.52 (d, J = 2.4 Hz, 1H), 7.37 (dd, J = 8.8, 2.4 Hz, 1H). ^{13}C NMR (100 MHz, $CDCl_3$, 298 K): δ (ppm) 178.8, 151.5, 139.7, 136.5, 129.9, 126.8, 126.1, 119.4, 118.7 (q, J = 319 Hz), 118.3. HR-MS (ESI-TOF) (m/z): $[M + H]^+$ calcd for $C_{14}H_8F_3O_4S_2$, 360.9811; found, 360.9801.

*9-Thioxo-9H-thioxanthen-3-yl Trifluoromethanesulfonate (**4**).* To a solution of compound **2** (3 g, 13.1 mmol) in anhydrous dichloromethane was added anhydrous pyridine (10.5 mL, 131.0 mmol), then trifluoromethanesulfonic anhydride (5.6 g, 19.8 mmol) was added dropwise under ice bath. After addition, the mixture was stirred at room temperature with argon atmosphere for 16 h. Then the solvent was removed, and the residue was dissolved in dichloromethane (150 mL). The solution was washed with 1 N HCl aqueous solution (100 mL) and brine (100 mL), and then the organic layer was dried over Na_2SO_4 and concentrated in vacuo. The crude product was purified by column chromatography (SiO_2, PE/EA = 100:1) to afford compound **2** (4.7 g, 95%) as a white solid. ^{1}H NMR (400 MHz, $CDCl_3$, 298 K): δ (ppm) 8.71 (d, J = 9.2 Hz, 1H), 8.61 (dd, J = 8.0 Hz, 1.2, 1H), 7.68 (m, 1H), 7.60 (dd, J = 8.0, 0.8 Hz, 1H), 7.54 (m, 1H), 7.52 (d, J = 2.4 Hz, 1H), 7.37 (dd, J = 8.8, 2.4 Hz, 1H). ^{13}C{^{1}H} NMR (100 MHz, $CDCl_3$, 298 K): δ (ppm) 178.8, 151.5, 139.7, 136.5, 129.9, 126.8, 126.1, 119.4, 118.7 (q, J = 319 Hz), 118.3. HR-MS (ESI-TOF) (m/z): $[M + H]^+$ calcd for $C_{14}H_8F_3O_4S_2$, 360.9811; found, 360.9801.

*(Z,E)-9-(8-Bromo-2-methyl-2,3-dihydro-1H-benzo[f]-thiochromen-1-ylidene)-9H-thioxanthen-3-yl Trifluoromethanesulfonate (**7**).* Compound **5**[24] (500 mg, 1.6 mmol) was dissolved in DMF and cooled under an ice bath, then iodosobenzene diacetate (509 mg, 1.6 mmol) was added slowly, the mixture was stirred for 5 min, compound **4** (588 mg, 1.6 mmol) was added. After that, the reaction solution was allowed to warm to room temperature and stirred for another 2 h. Then the solvent was removed under reduced pressure. The crude episulfide **6** was obtained as sticky liquid and used directly for the next step without further purification. The above crude episulfide **6** was dissolved in toluene, triphenylphosphine (839 mg, 3.2 mmol) was added, and then the mixture was heated under reflux for overnight. After that, the solvent was removed under reduced pressure, the residue was purified by column chromatography (SiO_2, PE/DCM = 20:1) to afford compound **7** (650 mg, 64%) as yellow powder, which was identified by ^{1}H NMR as a 44:56 mixture of cis/trans isomers. The isomers were used in the next step without further separation. ^{1}H NMR (400 MHz, $CDCl_3$, 298 K): δ (ppm) 7.72 (dd, J = 8, 2 Hz, 1H), 7.63 (d, J = 8.4 Hz, 1H), 7.58 (m, 1H), 7.52 (dd, J = 8.4, 2.4 Hz, 1H), 7.35–7.43 (m, 2H), 7.32 (d, J = 8.8 Hz, 1H), 7.27 (m, 1H), 7.08 (m, 1H), 6.83 (td, J = 7.6, 1.2 Hz, 1H), 6.50 (td, J = 7.6, 1.2 Hz, 1H), 6.37 (m, 1H), 4.04 (m, 1H), 3.69 (m, 1H), 3.10 (dd, J = 11.6, 2.8 Hz, 1H), 0.79 (d, J = 6.8 Hz, 3H). ^{13}C{^{1}H} NMR (100 MHz, $CDCl_3$, 298 K): δ (ppm) 147.5, 139.1, 137.5, 136.3, 136.0, 133.9, 133.7, 133.2, 132.6, 131.4, 130.8, 130.3, 129.7, 129.2, 129.0, 127.7, 126.8, 126.2, 125.8, 125.5, 120.6, 119.2, 118.8 (q, J = 305 Hz), 118.5, 36.9, 32.3, 19.1. HR-MS (ESI-TOF) (m/z): $[M + Na]^+$ calcd for $C_{28}H_{18}BrF_3O_3S_3Na$, 656.9446; found, 656.9448.

*(Z,E)-9-(8-Bromo-2-methyl-2,3-dihydro-1H-benzo[f]-thiochromen-1-ylidene)-9H-thioxanthen-3-ol (cis-**8**, trans-**8**).* To a solution of compound **7** (500 mg, 0.78 mmol) in dioxane was added tetraethylammonium hydroxide (229 mg, 1.56 mmol) aqueous solution (25%). The reaction mixture was stirred at room temperature for 2 h. Then the solvent was removed under reduced pressure, the residue was acidified with hydrochloric acid solution (1 N), and extracted with DCM (3 × 20 mL). The combined organic layer was washed with water (2 × 20 mL), brine (15 mL), and then the organic layer was dried over Na_2SO_4 and concentrated in vacuo. The crude product was purified by column chromatography (SiO_2, PE/EA = 50:1) to afford *cis*-**8** (194 mg, yield 49%) and *trans*-**7** (150 mg, yield 38%) as a white solid. *cis*-**8**: ^{1}H NMR (400 MHz, $CDCl_3$, 298 K): δ (ppm) 7.71 (d, J = 2 Hz, 1H), 7.60 (dd, J = 8.8 Hz, 1H), 7.56 (dd, J = 7.6, 1.2 Hz, 1H), 7.47 (t, J = 8.8 Hz, 1H), 7.37 (d, J = 8.8 Hz, 1H), 7.35 (td, J = 7.6, 1.2 Hz, 1H), 7.29 (dd, J = 7.6, 1.6 Hz, 1H), 6.25 (d, J = 8.4 Hz, 1H), 5.92 (dd, J = 8.4, 2.4 Hz, 1H), 4.09 (m, 1H), 3.72 (m, 1H), 3.10 (dd, J = 11.2, 2.8 Hz, 1H), 0.73 (d, J = 6.8 Hz, 3H). ^{13}C{^{1}H} NMR (100 MHz, $CDCl_3$, 298 K): δ (ppm) 154.8, 135.8, 135.7, 135.3, 134.9, 134.7, 132.2, 131.0, 0.9, 130.8, 129.6, 129.5, 129.2, 128.9, 128.2, 127.2, 127.2, 126.6, 126.3, 126.2, 126.1, 126.1, 112.8, 112.5, 36.4, 30.9, 22.0, 17.6, 13.0. HR-MS (ESI-TOF) (m/z): $[M - H]^-$ calcd for $C_{27}H_{18}BrOS_2$, 500.9988; found, 500.9997. *trans*-**8**: ^{1}H NMR (400 MHz, $CDCl_3$, 298 K): δ (ppm) 7.69 (d, J = 2 Hz, 1H), 7.48 (d, J = 8.4 Hz, 1H), 7.44 (d, J = 8.4 Hz, 1H), 7.40 (d, J = 6.8 Hz, 1H), 7.37 (d, J = 6.8 Hz, 1H), 7.29 (dd, J = 8, 0.8 Hz, 1H), 7.10 (d, J = 2.4 Hz, 1H), 7.04 (dd, J = 9.2, 2.4 Hz, 1H), 6.83 (dd, J = 8.4, 2.4 Hz, 1H), 6.78 (td, J = 7.6, 1.2 Hz, 1H), 6.44 (td, J = 7.6, 1.2 Hz, 1H), 6.37 (dd, J = 7.6, 1.2 Hz, 1H), 5.02 (s, 1H), 4.09 (m, 1H), 3.70 (m, 1H), 3.10 (dd, J = 11.2, 2.8 Hz, 1H), 0.76 (d, J = 6.8 Hz, 3H). ^{13}C{^{1}H} NMR (100 MHz, $CDCl_3$, 298 K): δ (ppm) 178.9, 154.4, 138.4, 137.5, 135.5, 135.2, 134.8, 133.9, 132.1, 130.9, 132.4, 131.5, 129.5, 129.0, 128.5, 127.5, 126.6, 126.4, 126.2, 126.0, 125.5, 124.5, 118.3, 114.4, 113.7, 37.2, 29.7, 19.2. HR-MS (ESI-TOF) (m/z): $[M - H]^-$ calcd for $C_{27}H_{18}BrOS_2$, 500.9988; found; 500.9998.

*tert-Butyl(5-((12-azidododecyl)amino)-5-oxopentyl)(3,5-di-tert-butylbenzyl)carbamate (**11**).* To a solution of compound **9**[25] (2.0 g, 4.7 mmol) in anhydrous dichloromethane was added compound **10**[26] (1.2 g, 4.7 mmol), a catalytic amount of DMAP, then EDCI (1.8 g, 9.5 mmol) was added dropwise under ice bath. After addition, the mixture was stirred at room temperature with argon atmosphere for 16 h. Then the solution was extracted with DCM (3 × 100 mL) and brine (100 mL), the organic layer was dried over Na_2SO_4 and concentrated in vacuo. The crude product was purified by column chromatography (SiO_2, PE/EA = 100:1) to afford compound **11** (2.4 g, 80%) as a transparent oil. ^{1}H NMR (400 MHz, $CDCl_3$, 298 K): δ (ppm) 7.31 (s, 1H), 7.05 (s, 2H), 4.37 (m, 2H), 3.22 (m, 4H), 2.17 (m, 2H), 1.75 (m, 2H), 1.53–1.66 (m, 8H), 1.39–1.53 (m, 9H), 1.29–1.33 (m, 18H), 1.20–1.29 (m, 16H). ^{13}C{^{1}H} NMR (100 MHz, $CDCl_3$, 298 K): δ (ppm) 172.9, 155.9, 150.8, 137.5, 121.6, 121.3, 121.0, 79.5, 51.4, 45.3, 39.4, 35.9, 34.7, 31.4, 29.6, 29.4, 29.4, 29.4, 29.2, 29.0, 28.7, 28.4, 27.9, 26.9, 26.8, 26.6, 22.9. HR-MS (ESI-TOF) (m/z): $[M + Na]^+$ calcd for $C_{37}H_{65}N_5O_3Na$, 650.4980; found, 650.4986.

*5-((12-Azidododecyl)amino)-N-(3,5-di-tert-butylbenzyl)-5-oxopentan-1-aminium Hexafluorophosphate(V) (**12**).* To a solution of compound **11** (2.0 g, 3.2 mmol) in dichloromethane was added TFA (5.3 g, 47 mmol). After addition, the mixture was stirred at room temperature under argon atmosphere for 3 h, the solvent was

DOI: 10.1021/acs.joc.9b00783
J. Org. Chem. 2019, 84, 5790–5802

removed under reduced pressure. Then to a solution of the residue in methanol was added saturated aqueous solution of NH_4PF_6 (100 mL), a white precipitate appeared quickly, the solution turned into milky white, the mixture was stirred vigorously for 30 min. The solvent was removed, the residue was extracted with DCM and washed with distilled water. The organic layer was collected and dried over Na_2SO_4, after concentrating in vacuo, compound **12** was obtained (2.0 g, 95%) as a transparent oil without further purification. ^{1}H NMR (400 MHz, CD_3CN, 298 K): δ (ppm) 7.46 (s, 1H), 7.35 (s, 1H), 7.34 (s, 1H), 4.13 (s, 2H), 3.24 (t, J = 6.8 Hz, 2H), 3.14 (m, 2H), 3.08 (t, J = 6.4 Hz, 2H), 2.24 (t, J = 6.0 Hz, 2H), 1.62−1.88 (m, 4H), 1.54−1.62 (m, 2H), 1.41−1.53 (m, 4H), 1.31 (s, 18H), 1.20−1.28 (m, 16H). ^{13}C{^{1}H} NMR (100 MHz, CD_3CN, 298 K): δ (ppm) 174.2, 151.7, 130.4, 124.2, 123.4, 52.0, 51.0, 46.5, 39.3, 34.6, 32.9, 29.2, 29.2, 29.1, 28.9, 28.9, 28.7, 28.4, 26.5, 26.3, 24.9, 19.8. HR-MS (ESI-TOF) (m/z): [M − PF_6^-]$^+$ calcd for $C_{32}H_{58}N_5O$, 528.4636; found, 528.4651.

Syntheses of Target Compound *cis*-18H$^+$, *trans*-18H$^+$ and Reference Compound *cis*-21H$^+$. ***cis*-14, *trans*-14.** To a solution of *cis*-**8** (450 mg, 0.79 mmol) in DMF was added a compound **13**[27] (689 mg, 1.2 mmol), potassium carbonate (331 mg, 2.4 mmol), and tetrakis (triphenylphosphine) palladium (91 mg, 0.079 mmol). After addition, the mixture was stirred at reflux under argon atmosphere for 8 h. The solvent was removed under reduced pressure, and then the residue was acidified with hydrochloric acid solution (1 N) and extracted with DCM (3 × 20 mL). The combined organic layer was washed with water (2 × 20 mL) and brine (15 mL), and then the organic layer was dried over Na_2SO_4 and concentrated in vacuo. The crude product was purified by column chromatography (SiO_2, DCM/methanol = 100:1) to afford *cis*-**14** as a white solid (480 mg, yield 70%). ^{1}H NMR (400 MHz, $CDCl_3$, 298 K): δ (ppm) 7.66 (d, J = 1.2 Hz, 1H), 7.61 (d, J = 7.6 Hz, 2H), 7.56 (d, J = 7.6 Hz, 2H), 7.37 (d, J = 8.4 Hz, 1H), 7.32 (td, J = 7.6, 0.8 Hz, 1H), 7.22 (m, 2H), 7.10 (m, 2H), 6.80−6.93 (m, 6H), 6.22 (d, J = 8.4 Hz, 1H), 5.93 (dd, J = 8.4, 2.0 Hz, 1H), 4.18 (m, 2H), 4.04−4.15 (m, 7H), 3.60−3.91 (m, 17H), 3.10 (dd, J = 11.2, 2.4 Hz, 1H), 0.78 (d, J = 6.8 Hz, 3H). ^{13}C{^{1}H} NMR (100 MHz, $CDCl_3$, 298 K): δ (ppm) 154.9, 152.0, 148.9, 148.8, 148.6, 136.6, 136.4, 136.0, 135.3, 135.2, 134.6, 132.3, 131.7, 131.4, 130.1, 129.8, 127.8, 127.5, 127.4, 126.0, 126.0, 125.2, 124.9, 121.7, 120.3, 114.3, 113.6, 113.1, 70.5, 70.4, 69.5, 69.4, 69.3, 37.3, 29.7, 19.2. HR-MS (ESI-TOF) (m/z): [M + Na]$^+$ calcd for $C_{51}H_{50}O_9S_2Na$, 893.2788; found, 893.2818. *trans*-**14** was prepared according to the same procedure as above. *trans*-**14**: ^{1}H NMR (400 MHz, $CDCl_3$, 298 K): δ (ppm): 7.59 (d, J = 1.6 Hz, 1H), 7.53 (d, J = 8.8 Hz, 1H), 7.48 (d, J = 8.4 Hz, 1H), 7.33 (d, J = 8.4 Hz, 1H), 7.30 (d, J = 8.4 Hz, 1H), 7.12 (dd, J = 8.8, 2.0 Hz, 2H), 7.07 (d, J = 2.4 Hz, 1H), 7.00 (s, 2H), 6.75−6.90 (m, 7H), 6.57 (s, 1H), 6.23−6.37 (m, 2H), 4.04−4.14 (m, 8H), 4.02 (m, 1H), 3.66−3.92 (m, 16H), 3.61 (m, 1H), 3.01 (dd, J = 11.2, 2.8 Hz, 2H), 0.69 (d, J = 6.8 Hz, 3H). ^{13}C{^{1}H} NMR (100 MHz, $CDCl_3$, 298 K): δ (ppm) 162.8, 153.3, 148.9, 138.7, 137.2, 135.3, 134.0, 131.7, 129.0, 128.5, 127.8, 127.6, 126.4, 125.4, 125.0, 124.7, 121.5, 114.4, 114.0, 113.1, 71.3, 69.9, 69.6, 69.36, 37.26, 36.7, 19.0. HR-MS (ESI-TOF) (m/z): [M + Na]$^+$ calcd for $C_{51}H_{50}O_9S_2Na$, 893.2788; found, 893.2794.

***cis*-16, *trans*-16.** To a solution of *cis*-**14** (200 mg, 0.23 mmol) in CH_3CN was added compound **15**[28] (82 mg, 0.34 mmol) and potassium carbonate (95 mg, 0.69 mmol). After addition, the mixture was stirred at reflux under argon atmosphere for 8 h. After the solvent was removed under reduced pressure, the residue was extracted with DCM (3 × 50 mL) and washed with brine (50 mL), water (50 mL), and then the organic layer was dried over Na_2SO_4 and concentrated in vacuo. The crude product was purified by column chromatography (SiO_2, DCM/methanol = 100:1) to afford *cis*-**16** as a white powder (183 mg, yield 85%). *trans*-**15** was prepared according to the same procedure as above. *cis*-**16**: ^{1}H NMR (400 MHz, CD_3Cl, 298 K): δ (ppm) 7.69 (d, J = 1.6 Hz, 1H), 7.54−7.65 (m, 4H), 7.38 (d, J = 8.4 Hz, 1H), 7.35 (td, J = 7.6, 1.2 Hz, 1H), 7.29 (dd, J = 7.6, 1.2 Hz, 1H), 7.24 (dd, J = 9.2, 1.2 Hz, 1H), 7.10 (m, 2H), 6.86 (d, J = 2.8 Hz, 1H), 6.86−6.91 (m, 4H), 6.92 (d, J = 8.8 Hz, 1H), 6.34 (d, J = 8.8 Hz, 1H), 6.00 (dd, J = 8.8, 2.8 Hz, 1H), 4.24 (t, J = 4.4 Hz, 2H), 4.13−4.21 (m, 6H), 4.11 (m, 1H), 3.89−3.98 (m, 8H), 3.80−3.88 (m, 8H), 3.69−3.79 (m, 3H), 3.11 (dd, J = 11.2, 2.8 Hz, 1H), 2.14 (td, J = 7.2, 2.8 Hz, 2H), 1.85 (t, J = 2.8 Hz, 1H), 1.72 (t, J = 2.4 Hz, 2H), 0.78 (d, J = 6.8 Hz, 3H). HR-MS (ESI-TOF) (m/z): [M + Na]$^+$ calcd for $C_{56}H_{56}O_9S_2Na$, 959.3258; found, 959.3263. ^{13}C{^{1}H} NMR (100 MHz, $CDCl_3$, 298 K): δ (ppm) 157.4, 149.0, 148.8, 148.4, 138.5, 137.4, 136.2, 135.6, 134.5, 134.2, 133.8, 132.0, 131.6, 131.2, 129.8, 128.9, 128.6, 128.4, 127.6, 127.5, 127.4, 126.3, 126.6, 126.0, 125.8, 125.4, 125.0, 124.8, 124.3, 124.6, 121.4, 119.9, 114.1, 114.0, 113.1, 112.9, 83.2, 71.2, 69.8, 69.5, 69.4, 69.3, 69.0, 66.3, 37.0, 31.9, 29.6, 27.9, 19.1, 15.0. *trans*-**16**: ^{1}H NMR (400 MHz, $CDCl_3$, 298 K): δ (ppm) 7.67 (d, J = 1.6 Hz, 1H), 7.62 (d, J = 8.4 Hz, 1H), 7.56 (d, J = 8.8 Hz, 1H), 7.50 (d, J = 8.4 Hz, 1H), 7.38 (d, J = 8.4 Hz, 1H), 7.27 (d, J = 7.6 Hz, 1H), 7.21 (dd, J = 8.8, 1.6 Hz, 1H), 7.18 (d, J = 6.8 Hz, 1H), 7.11 (m, 2H), 6.83−6.95 (m, 6H), 6.71 (m, 1H), 6.38 (m, 2H), 4.23 (m, 2H), 3.80−3.88 (m, 6H), 3.73 (m, 1H), 3.11 (dd, J = 11.2, 2.8 Hz, 1H), 2.44 (td, J = 7.2, 2.8 Hz, 2H), 2.04 (m, 2H), 2.00 (t, J = 2.8 Hz, 1H), 1.72 (m, 2H), 0.80 (d, J = 6.8 Hz, 3H). ^{13}C{^{1}H} NMR (100 MHz, $CDCl_3$, 298 K): δ (ppm) 157.4, 149.0, 148.8, 148.4, 138.5, 137.4, 136.2, 135.6, 134.5, 133.8, 132.0, 131.6, 131.2, 129.8, 128.9, 128.6, 128.3, 127.5, 127.4, 126.3, 126.0, 125.8, 125.6, 125.0, 124.8, 124.7, 119.9, 114.1, 114.0, 113.1, 112.9, 83.3, 71.2, 69.5, 69.4, 69.3, 69.0, 66.3, 37.1, 31.9, 29.6, 28.0, 18.9, 15.1. HR-MS (ESI-TOF) (m/z): [M + Na]$^+$ calcd for $C_{56}H_{56}O_9S_2Na$, 959.3258; found, 959.3261.

***cis*-17H$^+$, *trans*-17H$^+$.** To a solution of *cis*-**16** (100 mg, 0.106 mmol) in DCM (10 mL) was added compound **12** (72 mg, 0.106 mmol), the mixture was stirred at room temperature for 30 min. Then the solution was diluted to 250 mL with DCM, and $Cu(CH_3CN)_4PF_6$ (40 mg, 0.106 mmol) was added. After that, the reaction solution was stirred at room temperature under argon atmosphere for 24 h. The solution was extracted with DCM (3 × 50 mL) and distilled water (50 mL), then the organic layer was dried over Na_2SO_4 and concentrated in vacuo. The crude product was purified by column chromatography (SiO_2, DCM/MeOH = 100:1) to afford compound *cis*-**17H**$^+$ (94 mg, 30%) as a white solid. *trans*-**17H**$^+$ was prepared according to the same procedure as mentioned above. *cis*-**17H**$^+$: ^{1}H NMR (400 MHz, CD_3CN, 298 K): δ (ppm) 7.80 (s, 1H), 7.69 (d, J = 8.4 Hz, 1H), 7.65 (d, J = 7.6 Hz, 1H), 7.64 (dd, J = 8.4, 1.2 Hz, 1H), 7.62 (d, J = 8.4 Hz, 1H), 7.60 (d, J = 8.4 Hz, 1H), 7.37−7.50 (m, 4H), 7.31−7.37 (m, 2H), 7.23−7.27 (m, 4H), 7.04−7.13 (m, 1H), 6.99−7.13 (m, 1H), 6.81−6.97 (m, 6H), 6.28 (dd, J = 8.4, 1.6 Hz, 1H), 5.96 (dd, J = 8.4, 2.0 Hz, 1H), 4.66 (m, 2H), 4.24 (m, 2H), 4.02−4.21 (m, 9H), 3.92−4.01 (m, 1H), 3.76−3.91 (m, 4H), 3.69−3.76 (m, 4H), 3.67 (m, 2H), 3.55−3.67 (m, 4H), 3.54−3.40 (m, 4H), 3.34−3.20 (m, 4H), 3.11 (dd, J = 11.2, 2.8 Hz, 1H), 3.05 (m, 2H), 2.56 (m, 2H), 1.88 (m, 2H), 1.78 (m, 2H), 1.50 (m, 2H), 1.17−1.23 (m, 16H), 1.09−1.17 (m, 18H), 0.69 (d, J = 6.8 Hz, 3H). ^{13}C{^{1}H} NMR (100 MHz, CD_3CN, 298 K): δ (ppm) 171.7, 157.0, 151.1, 147.8, 147.7, 147.4, 147.0, 136.1, 135.8, 135.7, 135.7, 135.2, 133.8, 131.8, 131.6, 130.8, 129.7, 129.6, 127.6, 127.6, 127.5, 126.9, 126.6, 125.8, 124.9, 124.7, 124.6, 124.1, 123.9, 123.3, 121.3, 119.6, 119.6, 118.7, 112.9, 112.5, 112.0, 111.9, 111.2, 111.1, 70.4, 70.2, 70.0, 69.2, 68.2, 68.0, 67.1, 52.5, 49.5, 49.5, 48.5, 38.6, 36.6, 34.7, 34.3, 33.1, 31.6, 30.8, 29.6, 29.5, 29.4, 29.0, 28.5, 28.4, 28.3, 27.9, 26.7, 26.1, 25.7, 25.5, 24.6, 22.3, 21.5, 18.0. HR-MS (ESI-TOF) (m/z): [M − PF_6^-]$^+$ calcd for $C_{88}H_{114}N_5O_{10}S_2$, 1464.8002; found, 1464.8013. *cis*-**17H**$^+$: ^{1}H NMR (400 MHz, CD_3CN, 298 K): δ (ppm) 7.87 (s, 1H), 7.70 (d, J = 8.8 Hz, 1H), 7.62 (m, 2H), 7.53 (d, J = 8.4 Hz, 1H), 7.45 (s, 1H), 7.44 (m, 1H), 7.40 (m, 1H), 7.39 (d, J = 1.2 Hz, 1H), 7.30 (d, J = 8.0 Hz, 1H), 7.27 (m, 1H), 7.25 (d, J = 1.2 Hz, 1H), 7.22 (dd, J = 8.4, 2.4 Hz, 1H), 7.18 (s, 1H), 7.13 (dd, J = 8.4, 1.6 Hz, 1H), 7.06 (s, 1H), 7.01 (d, J = 9.6 Hz, 1H), 6.85−6.99 (m, 5H), 6.75 (m, 1H), 6.45 (m, 2H), 4.67 (t, J = 13.2 Hz, 1H), 4.42 (m, 2H), 4.29 (m, 2H), 4.13−4.22 (m, 4H), 4.10 (m, 1H), 3.94−4.09 (m, 4H), 3.90 (m, 1H), 3.67−3.87 (m, 10H), 3.40−3.67 (m, 4H), 3.32 (m, 2H), 3.20 (m, 1H), 3.14 (d, J = 11.2 Hz, 2H), 2.82 (m, 2H), 2.00 (m, 2H), 1.77 (m, 2H), 1.64 (m, 2H), 1.51 (m, 2H), 1.37 (m, 2H), 1.25−1.29 (m, 16H), 1.23 (d, J = 2.0 Hz, 18H), 0.67 (d, J = 6.4 Hz, 3H). ^{13}C{^{1}H} NMR (100 MHz, CD_3CN, 298 K): δ (ppm) 171.9, 164.0, 158.4, 151.9, 148.3, 147.6,

DOI: 10.1021/acs.joc.9b00783
J. Org. Chem. 2019, 84, 5790−5802

139.6, 138.1, 137.6, 136.2, 135.8, 134.9, 134.2, 133.6, 132.7, 132.6, 132.2, 131.3, 130.4, 129.3, 129.2, 129.0, 128.6, 128.3, 126.4, 125.4, 125.4, 125.3, 124.9, 124.9, 124.7, 124.1, 122.1, 120.2, 119.4, 115.3, 114.7, 113.6, 113.5, 113.5, 112.8, 112.0, 111.8, 71.1, 71.0, 70.9, 70.7, 70.7, 70.3, 69.1, 69.0, 68.7, 67.2, 53.2, 49.2, 39.4, 37.3, 35.2, 35.1, 32.2, 31.9, 31.2, 30.1, 29.9, 28.3, 27.3, 26.3, 23.0, 18.6. HR-MS (ESI-TOF) (m/z): $[M - PF_6^-]^+$ calcd for $C_{88}H_{114}N_5O_{10}S_2$, 1464.8002; found, 1464.7997.

*[1]Rotaxane cis-**18H**$^+$, [1]Rotaxane trans-**18H**$^+$.* To a solution of *cis*-**17H**$^+$ (90 mg, 0.056 mmol) in DCM (2 mL) was added excessive iodomethane (2 mL), the solution was kept in a pressure tube and sealed with a screw cap. Then the mixture was stirred at 40 °C for 24 h. After that, the solvent was removed under reduced pressure. Then to a solution of the residue in methanol was added saturated aqueous solution of NH_4PF_6 (100 mL), a white precipitate appeared quickly, the solution turned into milky white, the mixture was stirred vigorously for 30 min. Then the solvent was removed, the residue was extracted with DCM and washed with distilled water. The organic layer was collected and dried over Na_2SO_4, after concentrating in vacuo. The crude product was purified by column chromatography (SiO_2, DCM/MeOH = 100:1) to afford compound *cis*-**18H**$^+$ (80 mg, 80%) as a white solid. *trans*-**18H**$^+$ was prepared according to the same procedure as above. *cis*-**18H**$^+$: ^{1}H NMR (400 MHz, CD_3CN, 298 K): δ (ppm) 8.03 (d, J = 8.8 Hz, 1H), 7.86 (s, 1H), 7.72 (d, J = 8.8 Hz, 1H), 7.62−7.70 (m, 4H), 7.38−7.49 (m, 4H), 7.30−7.38 (m, 3H), 7.20−7.30 (m, 4H), 7.07−7.10 (m, 2H), 6.84−7.02 (m, 5H), 6.38 (d, J = 8.8 Hz, 1H), 6.18 (m, 1H), 6.02 (dd, J = 8.8, 2.8 Hz, 1H), 4.67 (m, 2H), 4.41 (m, 2H), 3.99−4.31 (m, 9H), 3.91 (s, 3H), 3.58−3.88 (m, 14H), 3.37−3.58 (m, 4H), 3.13 (dd, J = 11.2, 2.4 Hz, 1H), 3.01 (m, 2H), 2.73 (m, 2H), 2.04 (m, 2H), 1.87 (m, 2H), 1.26 (m, 2H), 1.14 (m, 2H), 0.68 (d, J = 6.8 Hz, 3H). ^{13}C{^{1}H} NMR (100 MHz, CD_2Cl_2, 298 K): δ (ppm) 172.0, 156.4, 151.3, 147.9, 147.6, 147.1, 145.7, 144.2, 138.8, 136.2, 135.7, 135.6, 135.2, 134.4, 132.7, 131.9, 131.8, 131.6, 130.9, 130.9, 130.0, 129.7, 128.4, 127.7, 127.5, 127.4, 126.7, 126.3, 125.9, 125.0, 124.6, 124.4, 124.1, 123.8, 123.3, 121.6, 120.1, 118.8, 118.6, 113.5, 113.2, 112.8, 112.6, 111.8, 111.6, 111.3, 70.5, 70.1, 68.7, 68.3, 68.1, 66.4, 51.4, 48.8, 45.3, 39.2, 37.1, 35.7, 35.1, 34.6, 33.6, 31.8, 31.0, 29.8, 29.6, 29.4, 29.3, 28.9, 28.7, 28.3, 28.0, 27.1, 26.5, 26.1, 25.9, 25.4, 24.8, 22.6, 20.2, 18.6. HR-MS (ESI-TOF) (m/z): $[M - PF_6^-]^+$ calcd for $C_{89}H_{117}F_6N_5O_{10}PS_2$, 1624.7878; found, 1624.7881, $[M - 2PF_6^-]^{2+}$ calcd for $C_{89}H_{117}N_5O_{10}S_2$, 739.9115; found, 739.9116. *trans*-**18H**$^+$: ^{1}H NMR (400 MHz, CD_3CN, 298 K): δ (ppm) 8.14 (d, J = 8.8 Hz, 1H), 7.87 (s, 1H), 7.72 (d, J = 8.8 Hz, 1H), 7.57 (t, J = 8.4 Hz, 2H), 7.48 (m, 1H), 7.44 (d, J = 4.0 Hz, 1H), 7.42 (d, J = 2.4 Hz, 1H), 7.40 (m, 1H), 7.35 (m, 1H), 7.31 (d, J = 7.6 Hz, 1H), 7.28 (d, J = 2.0 Hz, 1H), 7.26 (m, 2H), 7.24 (d, J = 2.4 Hz, 1H), 7.21 (m, 1H), 7.15 (d, J = 8.8, 2.4 Hz, 1H), 7.03 (d, J = 2.8 Hz, 1H), 7.02 (d, J = 2.8 Hz, 1H), 6.97 (m, 2H), 6.88−6.94 (m, 3H), 6.78 (m, 1H), 6.46 (m, 1H), 4.67 (m, 2H), 4.31−4.51 (m, 4H), 4.21 (m, 1H), 4.17 (d, J = 3.6 Hz, 2H), 4.15 (d, J = 3.6 Hz, 1H), 4.03−4.13 (m, 4H), 3.80−3.93 (m, 4H), 3.68−3.80 (m, 9H), 3.59−3.67 (m, 4H), 3.46 (m, 2H), 3.36 (m, 2H), 3.17 (m, 2H), 3.14 (m, 2H), 3.07 (m, 2H), 2.86 (m, 2H), 2.11 (m, 2H), 2.02 (m, 2H), 1.85 (m, 2H), 1.66 (m, 2H), 1.54 (m, 2H), 1.32−1.38 (m, 16H), 1.24 (s, 18H), 0.69 (d, J = 6.8 Hz, 3H). *trans*-**18H**$^+$: ^{1}H NMR (400 MHz, CD_3CN, 298 K): δ (ppm) 8.14 (d, J = 7.2 Hz, 1H), 7.87 (s, 1H), 7.72 (d, J = 8.8 Hz, 1H), 7.57 (t, J = 8.4 Hz, 2H), 7.47 (m, 1H), 7.44 (d, J = 4.4 Hz, 1H), 7.42 (d, J = 2.4 Hz, 1H), 7.40 (s, 1H), 7.35 (m, 1H), 7.31 (d, J = 7.6 Hz, 1H), 7.28 (m, 1H), 7.26 (m, 2H), 7.24 (d, J = 2.4 Hz, 1H), 7.21 (m, 1H), 7.15 (dd, J = 8.4, 2.4 Hz, 1H), 7.03 (d, J = 2.8 Hz, 1H), 7.02 (d, J = 2.8 Hz, 1H), 6.97 (m, 2H), 6.88−6.95 (m, 4H), 6.77 (m, 1H), 6.46 (m, 1H), 4.67 (m, 2H), 4.43 (m, 2H), 4.20−4.38 (m, 4H), 4.17 (d, J = 3.6 Hz, 2H), 4.15 (d, J = 3.6 Hz, 3H), 3.98−4.13 (m, 5H), 3.68−3.89 (m, 9H), 3.43−4.67 (m, 8H), 3.36 (m, 2H), 3.12−3.25 (m, 3H), 3.07 (m, 2H), 2.86 (m, 2H), 2.11 (m, 2H), 2.02 (m, 2H), 1.77−1.90 (m, 4H), 1.66 (m, 2H), 1.33−1.38 (m, 16H), 1.24 (s, 16H), 0.69 (d, J = 6.8 Hz, 3H). ^{13}C{^{1}H} NMR (100 MHz, CD_2Cl_2, 298 K): δ (ppm) 172.0, 156.4, 151.3, 147.9, 147.6, 147.3, 145.7, 144.2, 138.8, 136.2, 135.7, 135.6, 135.2, 134.4, 132.7, 131.9, 131.9, 131.8, 131.6, 130.9, 129.7, 128.4, 127.7, 127.5, 127.4, 126.7, 126.3, 125.9, 125.0, 124.6, 124.2, 123.8, 123.4, 121.6, 120.1, 118.7, 113.2, 112.7, 111.6, 111.3, 70.8, 70.5, 70.1, 68.7, 68.5, 68.3, 68.1, 66.4, 48.8, 39.2, 37.1, 35.7, 35.1, 34.6, 33.6, 31.8, 31.1, 31.0, 29.8, 29.4, 29.3, 28.9, 28.7, 28.3, 28.0, 27.1, 26.1, 25.9, 25.4, 22.6, 20.2, 18.6. HR-MS (ESI-TOF) (m/z): $[M - PF_6^-]^+$ calcd for $C_{89}H_{117}F_6N_5O_{10}PS_2$, 1624.7878; found, 1624.7866.

*cis-**19**.* To a solution of *cis*-**15** (100 mg, 0.068 mmol) in DCM (10 mL) was added compound **11** (46 mg, 0.068 mmol), the mixture was stirred at room temperature for 30 min. Then the solution was diluted to 250 mL with DCM, and $Cu(CH_3CN)_4PF_6$ (25 mg, 0.068 mmol) was added. After that, the reaction solution was stirred at room temperature under argon atmosphere for 24 h. Then the solution was extracted with DCM (3 × 50 mL) and distilled water (50 mL), the organic layer was dried over Na_2SO_4 and concentrated in vacuo. The crude product was purified by column chromatography (SiO_2, DCM/MeOH = 100:1) to afford compound *cis*-**19** (102 mg, 60%) as a transparent oil. ^{1}H NMR (400 MHz, $CDCl_3$, 298 K): δ (ppm) 7.92 (s, 1H), 7.77 (d, J = 5.2 Hz, 1H), 7.64−7.75 (m, 3H), 7.45−7.54 (m, 2H), 7.37−7.45 (m, 3H), 7.35 (s, 1H), 7.27 (s, 1H), 7.21 (d, J = 6.4 Hz, 1H), 7.17 (m, 2H), 6.90−7.06 (m, 6H), 6.40 (s, 1H), 6.36 (d, J = 6.8 Hz, 1H), 6.02 (d, J = 6.8 Hz, 1H), 4.43 (m, 2H), 4.05−4.33 (m, 10H), 3.82−3.98 (m, 9H), 3.68−3.70 (m, 9H), 3.49 (m, 2H), 3.16 (m, 3H), 2.62 (t, J = 6.0 Hz, 2H), 2.13 (m, 2H), 1.85 (m, 2H), 1.47−1.57 (m, 10H), 1.36−1.38 (m, 18H), 1.33−1.36 (m, 9H), 1.20−1.32 (m, 16H), 0.77 (d, J = 6.8 Hz, 3H). ^{13}C{^{1}H} NMR (100 MHz, $CDCl_3$, 298 K): δ (ppm) 172.2, 157.0, 150.7, 148.9, 148.7, 148.4, 146.3, 138.2, 136.1, 135.9, 135.6, 135.3, 135.0, 133.3, 131.8, 131.6, 130.8, 130.7, 129.7, 129.5, 127.6, 127.5, 126.8, 126.5, 125.7, 124.7, 124.6, 124.5, 123.7, 121.4, 121.3, 121.1, 120.8, 119.5, 118.7, 116.6, 114.1, 114.0, 112.7, 112.0, 78.8, 70.5, 69.4, 69.3, 68.9, 68.8, 68.7, 67.0, 54.2, 49.6, 49.5, 38.7, 36.6, 35.5, 34.4, 31.6, 31.5, 30.4, 29.9, 29.3, 29.1, 28.9, 28.6, 28.3, 27.6, 26.5, 26.0, 22.8, 22.3, 21.4, 18.1, 13.3. HR-MS (ESI-TOF) (m/z): $[M + Na]^+$ calcd for $C_{93}H_{121}N_5O_{12}S_2Na$, 1586.8345; found, 1586.8336.

*cis-**20**.* To a solution of *cis*-**19** (50 mg, 0.032 mmol) in DCM (2 mL) was added excessive iodomethane (2 mL), the solution was stay in a pressure tube and sealed with a screw cap. Then the mixture was stirred at 40 °C for 24 h. After that, the solvent was removed under reduced pressure. Then to a solution of the residue in methanol was added saturated aqueous solution of NH_4PF_6 (100 mL), a white precipitate appeared quickly, the solution turned into milky white, the mixture was stirred vigorously for 30 min. The solvent was removed, and the residue was extracted with DCM and washed with distilled water. The organic layer was collected and dried over Na_2SO_4, after concentrating in vacuo. The crude product was purified by column chromatography (SiO_2, DCM/MeOH = 100:1) to afford compound *cis*-**20** (27 mg, 50%) as a white solid. ^{1}H NMR (400 MHz, CD_3CN, 298 K): δ (ppm) 7.92 (s, 1H), 7.86 (d, J = 1.6 Hz, 1H), 7.70 (d, J = 8.8 Hz, 1H), 7.65 (m, 2H), 7.60 (d, J = 8.8 Hz, 1H), 7.44 (d, J = 7.2 Hz, 1H), 7.40 (d, J = 8.4 Hz, 1H), 7.28−7.37 (m, 3H), 7.23 (td, J = 8.4, 1.6 Hz, 1H), 7.19 (s, 1H), 7.15 (dd, J = 8.4, 2.8 Hz, 1H), 7.09 (d, J = 1.2 Hz, 1H), 6.96 (d, J = 8.4 Hz, 1H), 6.87−6.93 (m, 4H), 6.31 (s, 1H), 6.29 (d, J = 8.8 Hz, 1H), 5.95 (dd, J = 8.4, 2.4 Hz, 1H), 4.35 (s, 2H), 4.32 (d, J = 7.2 Hz, 1H), 4.21 (m, 2H), 4.13 (m, 2H), 4.10 (m, 4H), 4.05 (m, 1H), 3.89 (s, 3H), 3.76−3.87 (m, 9H), 3.75 (m, 2H), 3.64−3.72 (m, 8H), 3.14 (m, 2H), 3.11 (dd, J = 11.2, 2.4 Hz, 1H), 3.06 (m, 2H), 2.03 (m, 4H), 1.86 (m, 2H), 1.79 (m, 2H), 1.53 (m, 2H), 1.38−1.50 (m, 10H), 1.28−1.33 (m, 18H), 1.27 (s, 9H), 1.21−1.25 (m, 16H), 0.72 (d, J = 6.8 Hz, 3H). ^{13}C{^{1}H} NMR (100 MHz, CD_3CN, 298 K): δ (ppm) 159.8, 156.2, 150.5, 148.5, 148.4, 148.0, 143.6, 135.7, 135.6, 135.4, 135.0, 134.9, 133.1, 131.4, 131.0, 130.4, 130.4, 129.5, 129.5, 129.3, 127.4, 127.2, 127.2, 126.7, 126.4, 125.5, 124.5, 124.4, 124.3, 124.2, 123.5, 122.7, 121.1, 120.6, 119.2, 118.4, 113.8, 112.4, 112.3, 111.8, 78.6, 78.0, 77.6, 70.0, 70.0, 69.0, 69.0, 68.6, 68.4, 68.4, 66.2, 54.0, 53.2, 38.4, 36.8, 36.3, 35.2, 34.2, 31.3, 30.4, 30.3, 29.1, 29.0, 28.9, 28.7, 28.1, 27.4, 26.5, 26.3, 25.7, 25.2, 22.5, 22.1, 19.4, 17.7, 13.0. HR-MS (ESI-TOF) (m/z): $[M - PF_6^-]^+$ calcd for $C_{94}H_{124}N_5O_{12}S_2$, 1578.8682; found, 1578.8682.

*cis-**21H**$^+$.* To a solution of compound *cis*-**20** (100 mg, 0.064 mmol) in dichloromethane was added TFA (73 mg, 0.64 mmol). After

DOI: 10.1021/acs.joc.9b00783
J. Org. Chem. 2019, 84, 5790−5802

addition, the mixture was stirred at room temperature under argon atmosphere for 3 h, the solvent was removed under reduced pressure. Then to a solution of the residue in methanol was added saturated aqueous solution of NH_4PF_6 (5 mL), a white precipitate appeared quickly, the solution turned into milky white, the mixture was stirred vigorously for 30 min. The solvent was removed, and the residue was extracted with DCM and washed with distilled water. The organic layer was collected and dried over Na_2SO_4, after concentrating in vacuo, compound **21H**$^+$ was obtained (90 mg, 88%) as a white solid without further purification. ^{1}H NMR (400 MHz, CD_3CN, 298 K): δ (ppm) 7.91 (s, 1H), 7.82 (d, J = 1.6 Hz, 1H), 7.66 (d, J = 8.8 Hz, 1H), 7.59 (m, 3H), 7.37 (m, 2H), 7.34 (m, 1H), 7.23−7.32 (m, 4H), 7.21 (dd, J = 8.4 Hz, 2.0 Hz, 1H), 7.16 (td, J = 8.8, 2.0 Hz, 1H), 7.07 (dd, J = 8.4, 2.4 Hz, 1H), 7.01 (s, 2H), 6.97 (m, 2H), 6.92 (m, 2H), 6.82 (d, J = 2.4 Hz, 1H), 6.29 (d, J = 8.4 Hz, 1H), 6.24 (m, 1H), 5.93 (dd, J = 8.4, 2.4 Hz, 1H), 4.20−4.34 (m, 6H), 4.09−4.20 (m, 6H), 4.03 (m, 1H), 3.84 (s, 3H), 3.64−3.78 (m, 11H), 3.52−3.62 (m, 8H), 3.08 (m, 3H), 2.99 (m, 2H), 2.68 (d, J = 7.2 Hz, 2H), 1.96 (m, 4H), 1.71 (m, 4H), 1.47 (m, 4H), 1.29−1.42 (m, 16H), 1.20 (s, 18H), 0.61 (d, J = 6.8 Hz, 1H). ^{13}C{^{1}H} NMR (100 MHz, CD_3CN, 298 K): δ (ppm) 173.7, 156.7, 151.4, 148.0, 147.9, 147.6, 135.8, 135.4, 135.2, 135.1, 135.0, 134.6, 131.6, 131.4, 130.6, 130.2, 129.4, 127.4, 127.2, 126.7, 126.3, 125.6, 124.6, 124.4, 123.9, 123.0, 122.5, 122.4, 120.7, 115.8, 115.5, 114.2, 112.5, 111.7, 68.5, 68.3, 68.2, 68.0, 67.9, 67.8, 67.8, 67.4, 67.3, 67.3, 66.7, 54.0, 51.7, 49.3, 46.3, 39.0, 36.4, 34.3, 31.3, 30.6, 30.3, 29.6, 29.0, 28.9, 28.9, 28.8, 28.8, 28.7, 28.7, 28.5, 28.3, 28.0, 26.3, 25.7, 24.7, 22.1, 21.2, 19.9, 17.8, 13.1. HR-MS (ESI-TOF) (m/z): [M − 2PF_6^-]$^+$ calcd for $C_{89}H_{117}N_5O_{10}S_2$, 740.4132; found, 740.4136.

Syntheses of Reference [2]Rotaxane 24H$^+$ and 25H$^+$. *1,3-Dimethoxy-5-(pent-4-yn-1-yloxy)benzene (**22**).* To a solution of 3,5-dimethoxyphenol (500 mg, 3.25 mmol) in CH_3CN was added compound **15** (774 mg, 3.25 mmol) and potassium carbonate (449 mg, 3.25 mmol). After addition, the mixture was stirred at reflux under argon atmosphere for 8 h. Then the solvent was removed under reduced pressure, the residue was extracted with DCM (3 × 100 mL) and washed with brine (100 mL), water (100 mL), then the organic layer was dried over Na_2SO_4, and concentrated in vacuo. The crude product was purified by column chromatography (SiO_2, PE) to afford **22** as a white powder (608 mg, yield 85%). ^{1}H NMR (400 MHz, $CDCl_3$, 298 K): δ (ppm) 6.08 (m, 3H), 4.03 (t, J = 6.0 Hz, 2H), 3.77 (s, 6H), 2.40 (td, J = 7.2, 2.8 Hz, 2H), 1.98 (m, 3H). ^{13}C{^{1}H} NMR (100 MHz, $CDCl_3$, 298 K): δ (ppm) 161.4, 160.7, 93.3, 92.9, 83.4, 68.8, 66.1, 55.2, 28.0, 15.1. HR-MS (ESI-TOF) (m/z): [M + H]$^+$ calcd for $C_{13}H_{17}O_3$, 221.1172; found, 221.1155.

*[2]Rotaxane **24H**$^+$.* To a solution of **12** (100 mg, 0.148 mmol) in DCM (10 mL) was added compound **22** (33 mg, 0.148 mmol), compound **23**[29] (66 mg, 0.148 mmol) and $Cu(CH_3CN)_4PF_6$ (56 mg, 0.148 mmol). The mixture was stirred at room temperature under argon atmosphere for 24 h. Then the solution was extracted with DCM (3 × 50 mL) and distilled water (50 mL), the organic layer was dried over Na_2SO_4, and concentrated in vacuo. The crude product was purified by column chromatography (SiO_2, DCM/MeOH = 100:1) to afford compound **24H**$^+$ (158 mg, 80%) as a white solid. ^{1}H NMR (400 MHz, CD_2Cl_2, 298 K): δ (ppm) 7.21 (s, 1H), 7.17 (s, 1H), 7.15 (s, 2H), 6.70−6.80 (m, 8H), 5.84−5.94 (m, 3H), 5.52 (t, J = 5.6 Hz, 1H), 4.49 (m, 2H), 4.12 (m, 2H), 4.08 (m, 4H), 3.93 (m, 4H), 3.77 (t, J = 6.0 Hz, 1H), 3.65 (m, 4H), 3.58 (m, 4H), 3.56 (s, 6H), 3.44 (m, 4H), 3.23 (m, 4H), 3.01 (m, 2H), 2.91 (m, 2H), 2.68 (t, J = 7.6 Hz, 2H), 1.67 (m, 4H), 1.14−1.34 (m, 8H), 1.06−1.10 (m, 16H), 1.05 (s, 18H). ^{13}C{^{1}H} NMR (100 MHz, CD_2Cl_2, 298 K): δ (ppm) 171.8, 161.6, 160.9, 151.3, 147.6, 146.9, 131.7, 124.2, 123.4, 121.7, 120.9, 112.8, 93.3, 92.8, 70.6, 70.1, 68.3, 67.0, 55.3, 50.1, 48.8, 39.4, 35.1, 34.7, 31.1, 30.3, 29.7, 29.6, 29.5, 29.5, 29.4, 29.3, 29.3, 28.9, 26.9, 26.4, 26.0, 22.4, 22.0. HR-MS (ESI-TOF) (m/z): [M − PF_6^-]$^+$ calcd for $C_{69}H_{106}N_5O_{12}$, 1196.7833; found, 1196.7847.

*[2]Rotaxane **25H**$^+$.* To a solution of **24H**$^+$ (50 mg, 0.037 mmol) in DCM (2 mL) was added excessive iodomethane (2 mL), the solution was stayed in a pressure tube and sealed with a screw cap. Then the mixture was stirred at 40 °C for 24 h. After that, the solvent was removed under reduced pressure. Then to a solution of the residue in methanol (2 mL) was added saturated aqueous solution of NH_4PF_6 (2 mL), a white precipitate appeared quickly, the solution turned into milky white, the mixture was stirred vigorously for 30 min. The solvent was removed, and the residue was extracted with DCM (3 × 50 mL) and washed with distilled water (50 mL). The organic layer was collected and dried over Na_2SO_4, after concentrating in vacuo. The crude product was purified by column chromatography (SiO_2, DCM/MeOH = 80:1) to afford compound **25H**$^+$ (41 mg, 50%) as a white solid. ^{1}H NMR (400 MHz, CD_3CN, 298 K): δ (ppm): 8.15 (s, 1H), 7.39 (s, 1H), 7.29 (d, J = 1.6 Hz, 2H), 7.25 (m, 2H), 7.03 (s, 2H), 6.85−6.98 (m, 8H), 6.11 (s, 1H), 6.10 (s, 1H), 6.06 (d, J = 2.0 Hz, 2H), 4.67 (m, 2H), 4.45 (t, J = 7.2 Hz, 2H), 4.13−4.23 (m, 4H), 4.10 (s, 3H), 4.08−4.10 (m, 2H), 3.99−4.08 (m, 4H), 3.78−3.87 (m, 4H), 3.73 (s, 6H), 3.67−3.72 (m, 4H), 3.59−3.66 (m, 4H), 3.51−3.45 (m, 4H), 3.24 (m, 2H), 3.03 (m, 2H), 2.98 (t, J = 7.2 Hz, 2H), 2.13 (m, 2H), 1.89 (m, 2H), 1.82 (t, J = 7.2 Hz, 2H), 1.46 (m, 2H), 1.34−1.46 (m, 4H), 1.21−1.30 (m, 16H), 1.18 (s, 18H). ^{13}C{^{1}H} NMR (100 MHz, CD_3CN, 298 K): δ (ppm) 171.2, 161.4, 160.2, 160.2, 150.8, 147.2, 143.9, 131.6, 127.5, 123.8, 123.1, 121.1, 117.0, 112.3, 92.9, 92.6, 70.2, 69.7, 67.8, 65.9, 54.7, 54.0, 53.3, 52.3, 48.3, 38.5, 37.0, 34.4, 34.1, 30.3, 29.0, 29.0, 28.9, 28.7, 28.6, 28.2, 26.3, 25.9, 25.4, 25.3, 22.1, 21.9, 19.49. HR-MS (ESI-TOF) (m/z): [M − PF_6^-]$^+$ calcd for $C_{70}H_{109}F_{12}N_5O_{12}P_2$, 1356.7709; found, 1356.7701, [M − 2PF_6^-]$^{2+}$ calcd for $C_{70}H_{109}N_5O_{12}$, 605.9031; found, 605.9025.

■ ASSOCIATED CONTENT

Supporting Information

The Supporting Information is available free of charge on the ACS Publications website at DOI: 10.1021/acs.joc.9b00783.

Details of synthetic route, ^{1}H, ^{13}C NMR, ^{1}H−^{1}H COSY, HMQC, HMBC, 2D ROESY and HR-MS spectra, and DFT calculation methods (PDF)

Crystallographic data for compound *cis*-**8** (CIF)

■ AUTHOR INFORMATION

Corresponding Author

*E-mail: dahui_qu@ecust.edu.cn.

ORCID

Xiao-Ming Cao: 0000-0002-4782-853X

He Tian: 0000-0003-3547-7485

Ben L. Feringa: 0000-0003-0588-8435

Da-Hui Qu: 0000-0002-2039-3564

Notes

The authors declare no competing financial interest.

■ ACKNOWLEDGMENTS

This work was supported by NSFC/China (grants 21790361, 21871084, 21672060, 21421004), Shanghai Municipal Science and Technology Major Project (grant no. 2018SHZDZX03), the International Cooperation Program of Shanghai Science and Technology Committee (17520750100), the Fundamental Research Funds for the Central Universities, and the Programme of Introducing Talents of Discipline to Universities (B16017). We thank the Research Center of Analysis and Test of East China University of Science and Technology for help on the material characterization. B.L.F. gratefully acknowledge support from the Netherlands Ministry of Education, Culture and Science (Gravitation program 024.001.035), and the European Research Council (Advanced Investigator grant no. 694345 to B.L.F.).

DOI: 10.1021/acs.joc.9b00783
J. Org. Chem. 2019, 84, 5790−5802

REFERENCES

(1) (a) Yasuda, R.; Noji, H.; Kinosita, K.; Yoshida, M. F1-ATPase Is a Highly Efficient Molecular Motor that Rotates with Discrete 120° Steps. *Cell* **1998**, *93*, 1117−1124. (b) Schliwa, M. *Molecular Motors*; Wiley-VCH: Weinheim, 2003. (c) Noji, H.; Yasuda, R.; Yoshida, M.; Kinosita, K. Direct observation of the rotation of F1-ATPase. *Nature* **1997**, *386*, 299−302.

(2) (a) Mallik, R.; Carter, B. C.; Lex, S. A.; King, S. J.; Gross, S. P. Cytoplasmic dynein functions as a gear in response to load. *Nature* **2004**, *427*, 649−652. (b) Schnitzer, M. J.; Visscher, K.; Block, S. M. Force production by single kinesin motors. *Nat. Cell Biol.* **2000**, *2*, 718−723. (c) Hirokawa, N.; Noda, Y.; Tanaka, Y.; Niwa, S. Kinesin superfamily motor proteins and intracellular transport. *Nat. Rev. Mol. Cell Biol.* **2009**, *10*, 682−696.

(3) (a) Cluzel, P.; Surette, M.; Leibler, S. An ultrasensitive bacterial motor revealed by monitoring signaling proteins in single cells. *Science* **2000**, *287*, 1652−1655. (b) Blair, D. F. How bacteria sense and swim. *Annu. Rev. Microbiol.* **1995**, *49*, 489−522. (c) Zhou, J.; Lloyd, S. A.; Blair, D. F. Electrostatic interactions between rotor and stator in the bacterial flagellar motor. *Proc. Natl. Acad. Sci. U.S.A.* **1998**, *95*, 6436−6441.

(4) (a) Kelly, T. R.; De Silva, H.; Silva, R. A. Unidirectional rotary motion in a molecular system. *Nature* **1999**, *401*, 150−152. (b) Koumura, N.; Zijlstra, R. W. J.; Van Delden, R. A.; Harada, N.; Feringa, B. L. Light-driven monodirectional molecular rotor. *Nature* **1999**, *401*, 152−155. (c) Lewandowski, B.; De Bo, G.; Ward, J. W.; Papmeyer, M.; Kuschel, S.; Aldegunde, M. J.; Gramlich, P. M. E.; Heckmann, D.; Goldup, S. M.; D'Souza, D. M.; Fernandes, A. E.; Leigh, D. A. Sequence-specific peptide synthesis by an artificial small-molecule machine. *Science* **2013**, *339*, 189−193. (d) Kassem, S.; van Leeuwen, T.; Lubbe, A. S.; Wilson, M. R.; Feringa, B. L.; Leigh, D. A. Artificial molecular motors. *Chem. Soc. Rev.* **2017**, *46*, 2592−2621. (e) Qu, D.-H.; Tian, H. Synthetic small-molecule walkers at work. *Chem. Sci.* **2013**, *4*, 3031−3035. (f) Bruns, C. J.; Stoddart, J. F. *The Nature of the Mechanical Bond*; Wiley-VCH: Weinheim, 2016. (g) Balzani, V.; Credi, A.; Venturi, M. *Molecular Devices and Machines: A Journey into the Nano World*; Wiley-VCH: Weinheim, Germany, 2008. (h) Sauvage, J. P. *Molecular Machines and Motors*; Springer-Verlag: Berlin, 2001.

(5) (a) Sauvage, J.-P. From Chemical Topology to Molecular Machines (Nobel Lecture). *Angew. Chem., Int. Ed.* **2017**, *56*, 11080−11093. (b) Stoddart, J. F. Mechanically Interlocked Molecules (MIMs)-Molecular Shuttles, Switches, and Machines (Nobel Lecture). *Angew. Chem., Int. Ed.* **2017**, *56*, 11094−11125. (c) Feringa, B. L. The Art of Building Small: From Molecular Switches to Motors (Nobel Lecture). *Angew. Chem., Int. Ed.* **2017**, *56*, 11060−11078. (d) Erbas-Cakmak, S.; Leigh, D. A.; McTernan, C. T.; Nussbaumer, A. L. Artificial molecular machines. *Chem. Rev.* **2015**, *115*, 10081−10206. (e) Coskun, A.; Banaszak, M.; Astumian, R. D.; Stoddart, J. F.; Grzybowski, B. A. Great expectations: can artificial molecular machines deliver on their promise? *Chem. Soc. Rev.* **2012**, *41*, 19−30. (f) Chang, J.-C.; Tseng, S.-H.; Lai, C.-C.; Liu, Y.-H.; Peng, S.-M.; Chiu, S.-H. Mechanically interlocked daisy-chain-like structures as multidimensional molecular muscles. *Nat. Chem.* **2017**, *9*, 128−134. (g) Ragazzon, G.; Baroncini, M.; Silvi, S.; Venturi, M.; Credi, A. Light-powered autonomous and directional molecular motion of a dissipative self-assembling system. *Nat. Nanotechnol.* **2015**, *10*, 70−75. (h) Zhang, Q.; Rao, S.-J.; Xie, T.; Li, X.; Xu, T.-Y.; Li, D.-W.; Qu, D.-H.; Long, Y.-T.; Tian, H. Muscle-like Artificial Molecular Actuators for Nanoparticles. *Chem* **2018**, *4*, 2670−2684. (i) Cui, J.-S.; Ba, Q.-K.; Ke, H.; Valkonen, A.; Rissanen, K.; Jiang, W. Directional Shuttling of a Stimuli-Responsive Cone-Like Macrocycle on a Single-State Symmetric Dumbbell Axle. *Angew. Chem., Int. Ed.* **2018**, *57*, 7809−7814.

(6) (a) Wang, J.; Feringa, B. L. Dynamic control of chiral space in a catalytic asymmetric reaction using a molecular motor. *Science* **2011**, *331*, 1429−1432. (b) Leigh, D. A.; Marcos, V.; Wilson, M. R. Rotaxane catalysts. *ACS Catal.* **2014**, *4*, 4490−4497. (c) Xue, M.; Yang, Y.; Chi, X.; Yan, X.; Huang, F. Development of pseudorotaxanes and rotaxanes: from synthesis to stimuli-responsive motions to applications. *Chem. Rev.* **2015**, *115*, 7398−7501. (d) Choi, S.; Kwon, T.-w.; Coskun, A.; Choi, J. W. Highly elastic binders integrating polyrotaxanes for silicon microparticle anodes in lithium ion batteries. *Science* **2017**, *357*, 279−283. (e) Ge, X.; He, Y.; Guiver, M. D.; Wu, L.; Ran, J.; Yang, Z.; Xu, T. Alkaline Anion-Exchange Membranes Containing Mobile Ion Shuttles. *Adv. Mater.* **2016**, *28*, 3467−3472. (f) Ambrogio, M. W.; Thomas, C. R.; Zhao, Y.-L.; Zink, J. I.; Stoddart, J. F. Mechanized Silica Nanoparticles: A New Frontier in Theranostic Nanomedicine. *Acc. Chem. Res.* **2011**, *44*, 903−913.

(7) (a) Berná, J.; Leigh, D. A.; Lubomska, M.; Mendoza, S. M.; Perze, E. M.; Rudolf, P.; Teobaldi, G.; Zerbetto, F. Macroscopic transport by synthetic molecular machines. *Nat. Mater.* **2005**, *4*, 704−710. (b) Zhu, K.; O'Keefe, C. A.; Vukotic, V. N.; Schurko, R. W.; Loeb, S. J. A molecular shuttle that operates inside a metal-organic framework. *Nat. Chem.* **2015**, *7*, 514−519. (c) Foy, J. T.; Li, Q.; Goujon, A.; Colard-Itté, J.-R.; Fuks, G.; Moulin, E.; Schiffmann, O.; Dattler, D.; Funeriu, D. P.; Giuseppone, N. Dual-light control of nanomachines that integrate motor and modulator subunits. *Nat. Nanotechnol.* **2017**, *12*, 540−545. (d) Iwaso, K.; Takashima, Y.; Harada, A. Fast response dry-type artificial molecular muscles with [c2]daisy chains. *Nat. Chem.* **2016**, *8*, 625−632. (e) Sagara, Y.; Karman, M.; Verde-Sesto, E.; Matsuo, K.; Kim, Y.; Tamaoki, N.; Weder, C. Rotaxanes as Mechanochromic Fluorescent Force Transducers in Polymers. *J. Am. Chem. Soc.* **2018**, *140*, 1584−1587.

(8) (a) Muraoka, T.; Kinbara, K.; Aida, T. Mechanical twisting of a guest by a photoresponsive host. *Nature* **2006**, *440*, 512−515. (b) Kai, H.; Nara, S.; Kinbara, K.; Aida, T. Toward long-distance mechanical communication: studies on a ternary complex interconnected by a bridging rotary module. *J. Am. Chem. Soc.* **2008**, *130*, 6725−6727.

(9) (a) Štacko, P.; Kistemaker, J. C. M.; van Leeuwen, T.; Chang, M. C.; Otten, E.; Feringa, B. L. Locked synchronous rotor motion in a molecular motor. *Science* **2017**, *356*, 964−968. (b) Uhl, E.; Thumser, S.; Mayer, P.; Dube, H. Transmission of Unidirectional Molecular Motor Rotation to a Remote Biaryl Axis. *Angew. Chem., Int. Ed.* **2018**, *57*, 11064−11068.

(10) (a) Okuno, E.; Hiraoka, S.; Shionoya, M. A synthetic approach to a molecular crank mechanism: toward intramolecular motion transformation between rotation and translation. *Dalton Trans.* **2010**, *39*, 4107−4116. (b) Wang, Y.; Tian, Y.; Chen, Y.-Z.; Niu, L.-Y.; Wu, L.-Z.; Tung, C.-H.; Yang, Q.-Z.; Boulatov, R. A light-driven molecular machine based on stiff stilbene. *Chem. Commun.* **2018**, *54*, 7991−7994.

(11) (a) van Delden, R. A.; ter Wiel, M. K. J.; Pollard, M. M.; Vicario, J.; Koumura, N.; Feringa, B. L. Unidirectional molecular motor on a gold surface. *Nature* **2005**, *437*, 1337−1340. (b) Carroll, G. T.; Pollard, M. M.; van Delden, R.; Feringa, B. L. Controlled rotary motion of light-driven molecular motors assembled on a gold film. *Chem. Sci.* **2010**, *1*, 97−101. (c) Kaleta, J.; Chen, J.; Bastien, G.; Dračínský, M.; Mašát, M.; Rogers, C. T.; Feringa, B. L.; Michl, J. Surface Inclusion of Unidirectional Molecular Motors in Hexagonal Tris(o-phenylene)cyclotriphosphazene. *J. Am. Chem. Soc.* **2017**, *139*, 10486−10498.

(12) (a) Li, Q.; Fuks, G.; Moulin, E.; Maaloum, M.; Rawiso, M.; Kulic, I.; Foy, J. T.; Giuseppone, N. Macroscopic contraction of a gel induced by the integrated motion of light-driven molecular motors. *Nat. Nanotechnol.* **2015**, *10*, 161−165. (b) Chen, J.; Leung, F. K.-C.; Stuart, M. C. A.; Kajitani, T.; Fukushima, T.; van der Giessen, E.; Feringa, B. L. Artificial muscle-like function from hierarchical supramolecular assembly of photoresponsive molecular motors. *Nat. Chem.* **2018**, *10*, 132−138.

(13) Eelkema, R.; Pollard, M. M.; Vicario, J.; Katsonis, N.; Ramon, B. S.; Bastiaansen, C. W. M.; Broer, D. J.; Feringa, B. L. Nanomotor rotates microscale objects. *Nature* **2006**, *440*, 163.

(14) (a) García-López, V.; Chen, F.; Nilewski, L.; Duret, G.; Aliyan, A.; Kolomeisky, A. B.; Robinson, J. T.; Wang, G.; Pal, R.; Tour, J. M. Molecular machines open cell membranes. *Nature* **2017**, *548*, 567−572. (b) van Dijken, D. J.; Chen, J.; Stuart, M. C. A.; Hou, L.; Feringa, B. L. Amphiphilic molecular motors for responsive aggregation in

DOI: 10.1021/acs.joc.9b00783
J. Org. Chem. 2019, 84, 5790−5802

water. *J. Am. Chem. Soc.* **2016**, *138*, 660−669. (c) Lubbe, A. S.; Böhmer, C.; Tosi, F.; Szymanski, W.; Feringa, B. L. Molecular Motors in Aqueous Environment. *J. Org. Chem.* **2018**, *83*, 11008−11018.
(15) (a) Evans, N. H.; Beer, P. D. Progress in the synthesis and exploitation of catenanes since the Millennium. *Chem. Soc. Rev.* **2014**, *43*, 4658−4683. (b) Meng, Z.; Han, Y.; Wang, L.-N.; Xiang, J.-F.; He, S.-G.; Chen, C.-F. Stepwise Motion in a Multivalent [2](3)Catenane. *J. Am. Chem. Soc.* **2015**, *137*, 9739−9745. (c) Zhang, L.; Stephens, A. J.; Nussbaumer, A. L.; Lemonnier, J.-F.; Jurček, P.; Vitorica-Yrezabal, I. J.; Leigh, D. A. Stereoselective synthesis of a composite knot with nine crossings. *Nat. Chem.* **2018**, *10*, 1083−1088. (d) Bruns, C. J.; Stoddart, J. F. Rotaxane-Based Molecular Muscles. *Acc. Chem. Res.* **2014**, *47*, 2186−2199.
(16) (a) Coutrot, F.; Busseron, E. A new glycorotaxane molecular machine based on an anilinium and a triazolium station. *Chem.—Eur. J.* **2008**, *14*, 4784−4787. (b) Waelès, P.; Clavel, C.; Fournel-Marotte, K.; Coutrot, F. Synthesis of triazolium-based mono- and tris-branched [1]rotaxanes using a molecular transporter of dibenzo-24-crown-8. *Chem. Sci.* **2015**, *6*, 4828−4836. (c) Meng, Z.; Xiang, J.-F.; Chen, C.-F. Directional molecular transportation based on a catalytic stopper-leaving rotaxane system. *J. Am. Chem. Soc.* **2016**, *138*, 5652−5658. (d) Chen, S.; Wang, Y.; Nie, T.; Bao, C.; Wang, C.; Xu, T.; Lin, Q.; Qu, D.-H.; Gong, X.; Yang, Y.; Zhu, L.; Tian, H. An Artificial Molecular Shuttle Operates in Lipid Bilayers for Ion Transport. *J. Am. Chem. Soc.* **2018**, *140*, 17992−17998. (e) Zhang, Z.-J.; Han, M.; Zhang, H.-Y.; Liu, Y. A Double-Leg Donor-Acceptor Molecular Elevator: New Insight into Controlling the Distance of Two Platforms. *Org. Lett.* **2013**, *15*, 1698−1701.
(17) (a) Bao, X.; Isaacsohn, I.; Drew, A. F.; Smithrud, D. B. Determining the Intracellular Transport Mechanism of a Cleft−[2]Rotaxane. *J. Am. Chem. Soc.* **2006**, *128*, 12229−12238. (b) Riss-Yaw, B.; Clavel, C.; Laurent, P.; Waelès, P.; Coutrot, F. The Importance of Length and Flexibility of Macrocycle-Containing Molecular Translocators for the Synthesis of Improbable [2]-Rotaxanes. *Chem.—Eur. J.* **2018**, *24*, 13659−13666. (c) Riss-Yaw, B.; Morin, J.; Clavel, C.; Coutrot, F. How Secondary and Tertiary Amide Moieties are Molecular Stations for Dibenzo-24-crown-8 in [2]Rotaxane Molecular Shuttles? *Molecules* **2017**, *22*, 2017.
(18) (a) Cantrill, S. J.; Fulton, D. A.; Heiss, A. M.; Pease, A. R.; Stoddart, J. F.; White, A. J. P.; Williams, D. J. The influence of macrocyclic polyether constitution upon ammonium ion/crown ether recognition processes. *Chem.—Eur. J.* **2000**, *6*, 2274−2287. (b) Smukste, I.; Smithrud, D. B. Structure−Function Relationship of Amino Acid−[2]Rotaxanes. *J. Org. Chem.* **2003**, *68*, 2547−2558.
(19) Qu, D.-H.; Feringa, B. L. Controlling Molecular Rotary Motion with a Self-Complexing Lock. *Angew. Chem., Int. Ed.* **2010**, *49*, 1107−1110.
(20) (a) Koumura, N.; Geertsema, E. M.; van Gelder, M. B.; Meetsma, A.; Feringa, B. L. Second Generation Light-Driven Molecular Motors. Unidirectional Rotation Controlled by a Single Stereogenic Center with Near-Perfect Photoequilibria and Acceleration of the Speed of Rotation by Structural Modification. *J. Am. Chem. Soc.* **2002**, *124*, 5037−5051. (b) Pollard, M. M.; Klok, M.; Pijper, D.; Feringa, B. L. Rate acceleration of light-driven rotary molecular motors. *Adv. Funct. Mater.* **2007**, *17*, 718−729.
(21) (a) Barton, D. H. R.; Willis, B. J. Olefin Synthesis by Twofold Extrusion Processes. *J. Chem. Soc. D* **1970**, 1225−1226. (b) Kellogg, R. M.; Wassenaar, S. Thiocarbonyl ylides. An approach to "tetravalent sulfur" compounds. *Tetrahedron Lett.* **1970**, *11*, 1987−1990. (c) Koumura, N.; Geertsema, E. M.; Meetsma, A.; Feringa, B. L. Light-driven molecular rotor: Unidirectional rotation controlled by a single stereogenic center. *J. Am. Chem. Soc.* **2000**, *122*, 12005−12006.
(22) Huisgen, R. 1,3-Dipolar Cycloadditions. Past and Future. *Angew. Chem., Int. Ed.* **1963**, *2*, 565−598. (b) Kolb, H. C.; Finn, M. G.; Sharpless, K. B. Click chemistry: diverse chemical function from a few good reactions. *Angew. Chem., Int. Ed.* **2001**, *40*, 2004−2021.
(23) Khan, S.; Bernad, P. L.; Korshun, V. A.; Southern, E. M.; Shchepinov, M. S. Synthesis of S-pixyl derivatives for mass spectrometric applications. *Synlett* **2005**, *16*, 2453−2456.
(24) Pizzolalto, S. f.; Collins, B. S. L.; van Leeuwen, T.; Feringa, B. L. Bifunctional Molecular Photoswitches Based on Overcrowded Alkenes for Dynamic Control of Catalytic Activity in Michael Addition Reactions. *Chem.—Eur. J.* **2017**, *23*, 6174−6184.
(25) Smukste, I.; Smithrud, D. B. Structure−Function Relationship of Amino Acid−[2]Rotaxanes. *J. Org. Chem.* **2003**, *68*, 2547−2558.
(26) Masseroni, D.; Mosca, S.; Mower, M. P.; Blackmond, D. G.; Rebek, J. Cavitands as reaction vessels and blocking groups for selective reactions in water. *Angew. Chem., Int. Ed.* **2016**, *55*, 8290−8293.
(27) Zhou, W.; Guo, Y.-J.; Qu, D.-H. Photodriven Clamlike Motion in a [3]Rotaxane with Two [2]Rotaxane Arms Bridged by an Overcrowded Alkene Switch. *J. Org. Chem.* **2013**, *78*, 590−596.
(28) Karabiyikoglu, S.; Merlic, C. A. Transannular [4 + 2] Cycloaddition Reactions of Cobalt-Complexed Macrocyclic Dienynes. *Org. Lett.* **2015**, *17*, 4086−4089.
(29) Wessels, H. R.; Gibson, H. W. Multi-gram syntheses of four crown ethers using K+ as templating agent. *Tetrahedron* **2016**, *72*, 396−399.

DOI: 10.1021/acs.joc.9b00783
J. Org. Chem. 2019, 84, 5790−5802